DISCLAIMER

This report was prepared as an account of work sponsored by an agency of the United States Government. Neither the United States Government nor any agency thereof, nor any of their employees, makes any warranty, express or implied, or assumes any legal liability or responsibility for the accuracy, completeness, or usefulness of any information, apparatus, product, or process disclosed, or represents that its use would not infringe privately owned rights. Reference herein to any specific commercial product, process, or service by trade name, trademark, manufacturer, or otherwise does not necessarily constitute or imply its endorsement, recommendation, or favoring by the United States Government or any agency thereof. The views and opinions of authors expressed herein do not necessarily state or reflect those of the United States Government or any agency thereof. Reference herein to any social initiative (including but not limited to Diversity, Equity, and Inclusion (DEI); Community Benefits Plans (CBP); Justice 40; etc.) is made by the Author independent of any current requirement by the United States Government and does not constitute or imply endorsement, recommendation, or support by the United States Government or any agency thereof.

ANL/NSE-24/48 Rev.1

Verification of the ENDF/B-VII.1 Based MC^2-3 Library

Nuclear Science and Engineering Division

ANL/NSE-24/48 Rev.1

Verification of the ENDF/B-VII.1 based MC^2-3 Library

prepared by

Changho Lee, Hansol Park, Zhaopeng Zhong
Nuclear Science and Engineering Division, Argonne National Laboratory

August 15, 2024

REVISION HISTORY

Revision No.	Date	Section(s) Affected	Description
0	August 2024	All	Initial Release (library v1.0) Verified by MC^2-3 v3.3.3
1	March 2025	Sections 4.2.1 and 4.2.2	Further verification of gamma heating rates

ABSTRACT

The MC^2-3 code, developed by Argonne National Laboratory under the DOE-NE NEAMS program, is a multigroup cross section generation code for fast reactor applications. Last year, the ENDF/B-VII.0 (E70) MC^2-3 library, which has been extensively used, verified, and validated over a long period, was intensively reverified and updated to support the commercial grade dedication (CGD) requirement of the TerraPower Natrium project. This year, the ENDF/B-VII.1 (E71) MC^2-3 library, the preliminary version of which was generated several years ago, was regenerated and rigorously verified to support the Natrium project as well as the completion of verification of the E71 library. The E71 library was verified using the process developed during the verification of the E70 library, including comparisons of cross sections with the NJOY-generated cross sections, comparisons of the resolved resonance cross sections with those using the PEDNF library, and comparison of total cross sections with the sum of partial cross sections. Additional verifications were conducted to ensure that the benchmark problem solutions with the E71 library are reasonable compared to the corresponding Monte Carlo solutions. Furthermore, the E71 gamma library was generated, which includes data for prompt gamma, delayed gamma, and delayed beta as well as neutron and gamma heating. The gamma library was verified at the level of individual isotopes. The EBR-II core solutions from MC^2-3/ DIF3D and MCNP were compared, demonstrating that those solutions in terms of k-effective and assembly powers were in good agreement.

TABLE OF CONTENTS

LIST OF FIGURES

LIST OF TABLES

1. Introduction

The MC^2-3 code [1, 2] is a multigroup cross section generation code for fast reactor applications, developed by Argonne National Laboratory (ANL) under the DOE-NE Nuclear Energy Advanced Modeling and Simulation (NEAMS) program. The code performs self-shielding of isotopic ultrafine group (UFG) cross sections based on material and geometry background cross sections and the narrow resonance (NR) approximation. It solves a homogeneous, one-dimensional or multi-dimensional transport equation in ultrafine or hyperfine groups to determine geometry background cross sections and accurately account for heterogeneity effects. For region-wise cross section generation, UFG regional spectra are generated from an external code, such as TWODANT [3], and used for group condensation to broad-group (BG) cross sections. Using the gamma library, the gamma data, including gamma interaction cross sections, gamma and neutron heating, and gamma yield data, are generated for a user-specified number of gamma groups.

For over a decade, the neutron and gamma libraries of MC^2-3 based on ENDF/B-VII.0 (E70) data [4] have been widely used for fast reactor design and analysis. Last year, the E70 library was intensively reverified and updated to meet the commercial grade dedication (CGD) requirements of the TerraPower Natrium project. [5] This year, the ENDF/B-VII.1 (E71) [6] MC^2-3 library, whose preliminary version was generated several years ago, has been regenerated and rigorously verified to support the Natrium project as well as complete the verification of the E71 library.

Many of the issues identified and resolved in the E70 library were applicable to the E71 library, which helped expedite the update process for the E71 library. In addition, the E71 library was verified using the process developed during the verification of the E70 library, including comparisons of cross sections with the NJOY [7]-generated cross sections, comparisons of the resolved resonance cross sections with those using the PENDF library, and comparison of total cross sections with the sum of partial cross sections. Further verifications were conducted to ensure that benchmark problem solutions with the E71 library are consistent with corresponding Monte Carlo solutions.

Furthermore, the E71 gamma library was generated, which includes data for prompt gamma, delayed gamma, and delayed beta as well as neutron and gamma heating. The gamma library was verified at the level of individual isotopes by comparing heating with MCNP [8] solutions. Additionally, the EBR-II core solutions from MC^2-3/DIF3D-VARIANT [9] (hereafter DIF3D) and MCNP were compared, demonstrating that those solutions in terms of k-effective and assembly powers were in good agreement.

All verification tests of the E71 library were performed using the latest version of MC^2-3, v3.3.3, which was released in November 2023. The initial production versions of the E71 neutron and gamma libraries are v1.1 and v1.0, respectively.

In this report, Section 2 outlines the updated Gitlab repository structures, Section 3 presents the generation and verification of the neutron library, and Section 4 focuses on discussing the

generation and verification of the gamma library. Finally, Section 5 presents the conclusions drawn from the investigation and highlights the key takeaways.

2. GitLab Repositories for MC^2-3

There are three GitLab repositories involved in the updates of the E71 neutron and gamma libraries: MC^2-3 sources and benchmarks, MC^2-3 libraries, and MC^2-3 verification. The E71 neutron and gamma libraries are saved in directories with the `.e71` extension: `lib.mcc.e71` and `lib.gamma.e71`. Each directory contains library files as well as a version file, which includes version identification: `version` for `lib.mcc.e71` and `typeversion` for `lib.gamma.e71`. The MC^2-3 library GitLab is mainly composed of the following directories.

Location: https://git-nse.egs.anl.gov/proteus/xs/mcc3_library

- lib.mcc.e70
- lib.mcc.e71
- lib.gamma.e70
- lib.gramma.e71

Verification test inputs and outputs are also saved in the MC^2-3 verification GitLab, which contains multiple directories as below. Among those directories, the `VVcases` directory includes fast reactor benchmark cases for LANL, ZPPR-15, ZPPR-21, ZPR-6, Monju, BFS, ABTR, etc., and the `LibraryTests` directory contains several typical fast reactor homogeneous cases based on CEFR, EBR-II and VTR core compositions Those cases were tested using the E71 library and compared with corresponding Monte Carlo solutions, which were regenerated using the E71 data. Details of the test results will be discussed in Section 3.

Location: https://git-nse.egs.anl.gov/proteus/xs/MCC3_verification

- Documents
- IOtests
- IntegralTests
- LibraryTests
    - ENDFB70
    - ENDFB71
        - 0DProblems
        - Heating
            - DIF3D
            - MCC3
            - MCNP
            - Script
- Scripts
- UnitTest
- VVcases
    - ENDFB70

        - MCC3DIF3D
        - MonteCarlo
    - ENDFB71
        - MCC3DIF3D
        - MonteCarlo

Additionally, the outputs of the benchmark problems used in the MC^2-3 main GitLab were updated. These updates ensure that the MC^2-3 outputs using the E71 libraries can be reproduced for any future changes to the sources and libraries.

Location: https://git-nse.egs.anl.gov/proteus/xs/mcc3

- benchmark
    - REF_OUTPUT_e71
    - REF_OUTPUT
    - REF_INPUT
- src
- doc

To run MC^2-3 for the benchmark problems, an additional Python script, named `run_benchmarks_e71.py` was created and is used as below. The Python script is basically the same as `run_benchmarks.py`, therefore these two scripts will be merged in the future. The E71 Python script creates the directory RESUTLS_e71 for E71.

- (For the E70 library) python run_benchmarks.py run
- (For the E71 library) python run_benchmarks_e71.py run

After completing all calculations, the following commands should be run to compare outputs with the reference files at REF_OUTPUT_e71.

- (For the E70 library) python run_benchmarks.py compare_results
- (For the E71 library) python run_benchmarks_e71.py compare_results

3. ENDF/B-VII.1-based MC^2-3 neutron library

The MC^2-3 neutron library includes a set of binary or ASCII files, as listed in Table **3-1** with their descriptions. Most of these files are generated by ETOE2 [10], while MCCF9 and MCCF10 are generated by NJOY and utility programs. Details will be discussed in the following sections.

Table 3-1 MC^2-3 library files

Files	Description
MCCF1	Maximum data sizes, control information, material IDs, etc.
MCCF2	Isotope-independent function table
MCCF3	Unresolved resonance data
MCCF4	Resolved resonance data
MCCF5	Ultrafine-group smooth cross section data
MCCF6	Inelastic and (n,2n) P_0 scattering data
MCCF7	Fission spectrum, neutron-per-fission data
MCCF8	T-function matrices, anisotropic elastic scattering Legendre data
MCCF9	Chi matrix, infinite-dilute ultrafine-group total cross sections
MCCF10	Ultrafine-group Inelastic scattering matrices
ADELAY	Delayed neutron data
version	Version number and description

3.1 Neutron Library Generation

Among the first eight files shown in Table 3-1, MCCF2 contains isotope-independent function tables that do not change with ENDF/B data, while the remaining seven files are generated by ETOE2.

Similarly to the E70 data, the E71 data commonly uses the multi-level Breit-Wigner (MLBW) and Reich-Moore (RM) formalisms to represent resolved resonances. These formalisms cover resolved resonances for almost all the isotopes except for Cl^{35}. Currently, ETOE-2 cannot correctly process the R-Matrix limited (RML) formalism. As a result, the cross sections for Cl^{35} are not precise but will be corrected in future updates.

The library generation of MC^2-3 using ETOE2 does include only certain reactions: total, capture (n,g), fission, nu-fission, elastic, inelastic, (n,2n), (n,p), (n,d), (n,t), (n,he3), (n,alpha). It does not process other reactions: (n,3n), (n,4n), (n,np), (n,nα), (n,t2α), etc., all of which are threshold reactions occurring in the energy range of several MeV. This limitation is related to an inherent limitation in the CCCC file format, including ISOTXS, which does not support these missing reactions.

As shown in Table 3.3, there are 60 isotopes noticeably affected by these issues, whether their magnitudes are small or relatively large. However, their impact on neutronics calculations is very minor. Figure 3.1 shows relatively large deviations in total cross sections between MC^2-3 and NJOY for B^{11} and F^{19} in the energy range over about 10 MeV, which are due to the missing processing of (n,t2α) and (n,nα) reactions, respectively.

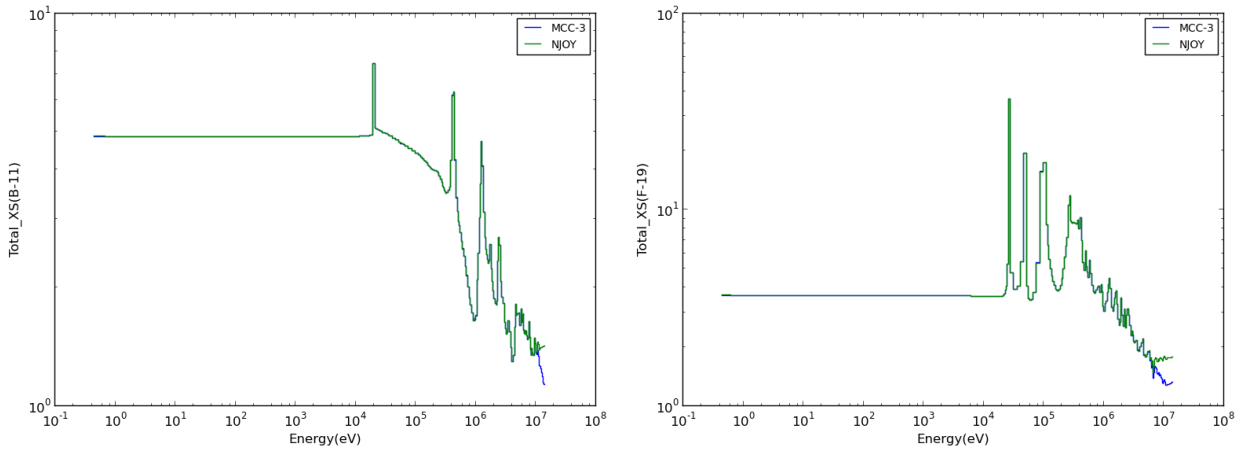

B^{11} F^{19}

Figure 3-1 230-group total cross sections from MC^2-3 and NJOY for B^{11} and F^{19}.

MCCF9 contains fission spectrum matrices and infinite-dilute ultrafine-group total cross sections, while MCCF10 involves inelastic scattering matrices up to P1. The isotopic fission spectrum matrices in MCCF9 are provided as a function of incident neutron energies because the fission spectrum data in MCCF7 are based on a single effective energy. Currently, the fission spectrum data for 68 isotopes (from Ra^{223} to Fm^{255}) and total cross sections for all 423 isotopes are included in MCCF9.

Inelastic scattering data are included in MCCF6, but they are limited to P0. Therefore, P1 inelastic scattering data, which are important to fast reactors, are obtained from MCCF10. The inelastic scattering matrices cross sections for all 423 isotopes are included in MCCF10.

The delayed neutron data in ADELAY has been updated by directly processing ENDF/B-VII.1 data. A utility program was updated to process the data (MT 451 and MT 455) and write them in the ADELAY ASCII format. As a result, 32 isotopes were processed and included in ADELAY, as shown in Table 3-2.

Table 3-2 Delayed neutron data in ADELAY based on ENDF/B-VII.1 data

1	Th-227	2	Th-229	3	Th-232	4	Pa-231	5	Pa-233
6	U-232	7	U-233	8	U-234	9	U-235	10	U-236
11	U-237	12	U-238	13	U-239	14	U-240	15	U-241
16	Np-237	17	Np-238	18	Pu-238	19	Pu-239	20	Pu-240
21	Pu-241	22	Pu-242	23	Am-241	24	Am-243	25	Cm-242
26	Cm-245	27	Cf-249	28	Cf-251	29	Cf-252	30	Es-254
31	Es-254m1	32	Fm-255						

Table 3-3 Reaction types not processed in the current ENDF/B-VII.0 library of MC^2-3.

Seq. No	Isotope	Reaction	Seq. No	Isotope	Reaction
1	B^{10}	(n,t2α)	31	Se^{74}	(n,np), (n,nα)
2	B^{11}	(n,nα)	32	Br^{79}	(n,np)
3	F^{19}	(n,nα)	33	Kr^{78}	(n,np)
4	Na^{22}	(n,nα)	34	Mo^{92}	(n,np)
5	Mg^{24}	(n,nα)	35	Ru^{96}	(n,np)
6	Al^{27}	(n,np)	36	Cd^{106}	(n,nα)
7	P^{31}	(n,np)	37	Ba^{140}	(n,3n)
8	S^{32}	(n,nα), (n,np)	38	Ce^{144}	(n,3n)
9	S^{33}	(n,nα), (n,np)	39	Ra^{223}	(n,3n)
10	S^{34}	(n,nα)	40	Ra^{224}	(n,3n)
11	Cl^{35}	(n,np), (n,nα)	41	Ra^{225}	(n,3n)
12	Cl^{37}	(n,np), (n,nα)	42	Ra^{226}	(n,3n)
13	Ar^{36}	(n,np), (n,nα)	43	Ac^{225}	(n,3n)
14	Ar^{38}	(n,nα), (n,np)	44	Ac^{226}	(n,3n)
15	K^{39}	(n,np), (n,nα)	45	Ac^{227}	(n,3n)
16	K^{40}	(n,np), (n,nα)	46	Th^{232}	(n,3n)
17	K^{41}	(n,np), (n,nα)	47	Th^{233}	(n,3n)
18	Ca^{40}	(n,np)	48	Th^{234}	(n,3n)
19	Ca^{42}	(n,np), (n,nα)	49	U^{240}	(n,3n)
20	Sc^{45}	(n,np), (n,nα)	50	U^{241}	(n,3n)
21	Ti^{46}	(n,np), (n,nα)	51	Pu^{243}	(n,3n)
22	Cr^{50}	(n,np), (n,nα)	52	Pu^{244}	(n,3n)
23	Fe^{54}	(n,np)	53	Pu^{246}	(n,3n)
24	Co^{58}	(n,np), (n,nα)	54	Cm^{248}	(n,3n)
25	Co^{58m}	(n,np), (n,nα)	55	Bk^{250}	(n,3n)
26	Co^{59}	(n,np)	56	Cf^{250}	(n,3n)
27	Ni^{58}	(n,np)	57	Cf^{251}	(n,3n)
28	Cu^{63}	(n,np)	58	Cf^{252}	(n,3n)
29	Zn^{64}	(n,np), (n,nα)	59	Cf^{254}	(n,3n)
30	Ge^{70}	(n,nα), (n,np)	60	Es^{254}	(n,3n)

* Only the meaningful reactions contributing the differences from NJOY are listed.
* (n,t2α): production of tritium and 2 alpha, (n,nα): production of neutron and alpha, (n,3n): production of 3 neutrons, (n,np): production of neutron and proton.

3.2 Verification

3.2.1 Library Assessment

The update and verification of the E71 library for MC^2-3 were initiated. As an initial step, the latest version of the E71 library was regenerated and evaluated to identify issues with individual isotopic cross sections. Three categories of verification tests were conducted to ensure that all isotopic cross sections were generated correctly: comparison of 230-group cross sections generated from MC^2-3 and NJOY, comparison of 230-group cross sections generated from MC^2-3 with the MCC library and PENDF libraries, and comparison of 230-group total cross sections and the sum of partial cross sections.

The comparison of 230-group isotopic cross sections generated from MC^2-3 and NJOY revealed noticeable discrepancies for several isotopes (Co^{58}, Tm^{168}, Zr^{90}, Cf^{249}, etc.). These issues were examined and mostly resolved by updating the ETOE2 code. Figure 3.2 shows isotopic average percentage errors in 230-group total cross sections for all 423 isotopes when comparing MC^2-3 and NJOY. A few isotopes (Cl^{35}, Ar^{40}, and Ni^{64}) exhibited errors greater than 0.5%. Among them, the large error for Cl^{35} is expected because we do not currently process RML-based resonance data. Part of the errors in Ar^{40} and Ni^{64} could be due to inconsistencies of the pointwise neutron spectra used by MC^2-3 and NJOY. This inconsistency may amplify the error in the resolved resonance energy range, in which the 230-group cross section is sensitive to the neutron spectra. The cross-section error for Ar^{40} and Ni^{64} in the resolved resonance energy range could be better demonstrated by using MC^2-3 with the PENDF library instead of NJOY.

An additional test was conducted by comparing the 230-group total cross sections in the resolved resonance energy range using MC^2-3 with its own and PENDF (generated by NJOY) libraries. This comparison is more consistent because the pointwise and same ultrafine group spectrum are used within MC^2-3, whereas in the previous comparison, MC^2-3 and NJOY used different spectra to determine the 230-group cross sections. In this comparison, only isotopes with resolved resonances were considered. As shown in Figure 3.3 , the percent errors of most of the 423 isotopes are under 1%.

Lastly, a consistency check of cross sections was conducted by comparing total cross sections with the sum of all partial cross sections of an isotope. As shown in Figure 3.4 , most of the 423 isotopes have discrepancies in 230-group cross sections that are acceptable (< 0.001 %), except for several isotopes (Ca^{40}, Ca^{48}, Zr^{95}, Cs^{136}, Pm^{148}, and Tm^{167}). Investigations will be conducted on those isotopes.

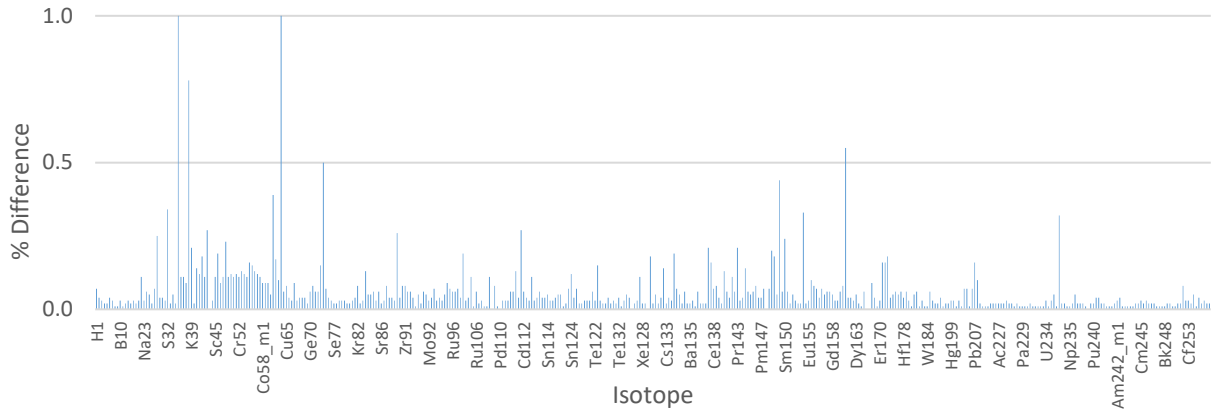

Figure 3-2 **Average % difference in the 230-group total cross sections for all 423 isotopes, generated from MC²-3 and NJOY with the ENDF/B-VII.1 library.**

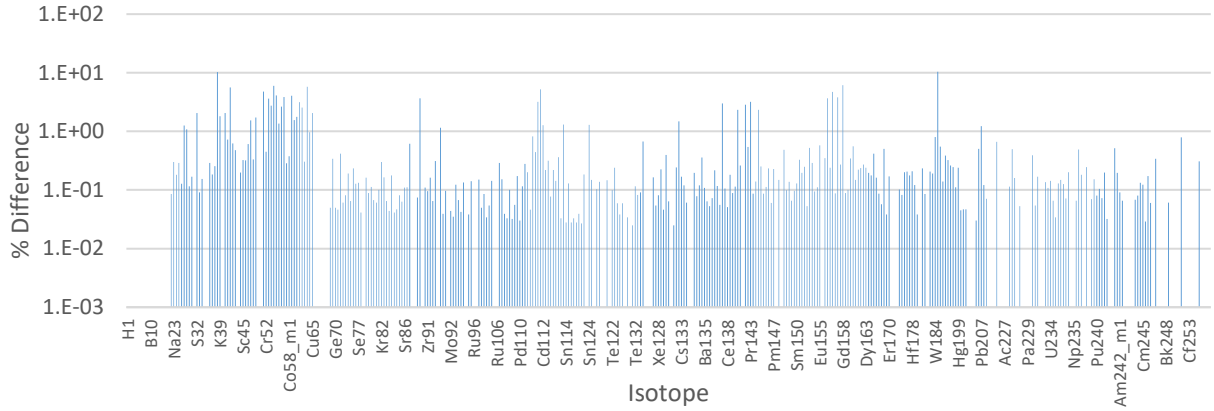

Figure 3-3 **Average % difference in the 230-group total cross sections for all 423 isotopes in the resolved resonance energy range, generated from MC²-3 using the MC²-3 and PENDF (NJOY) ENDF/B-VII.1 libraries.**

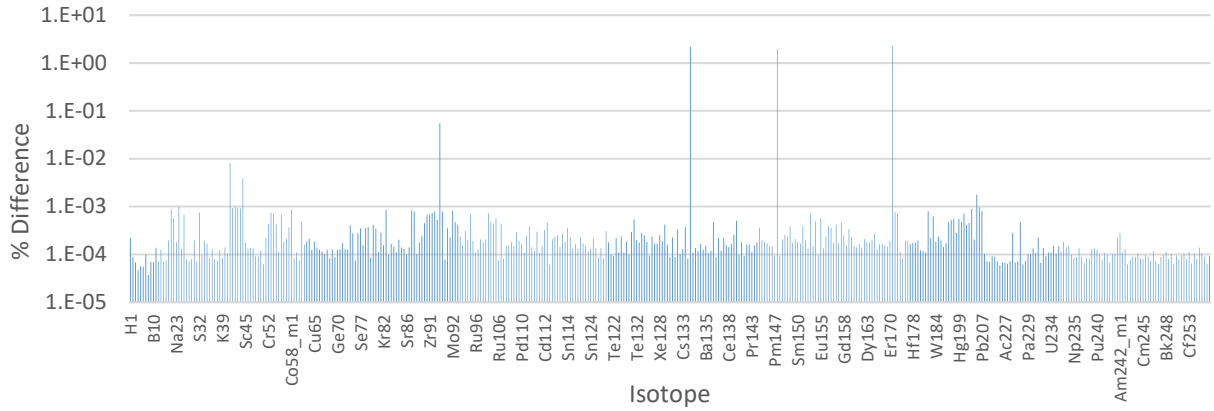

Figure 3-4 **% differences between the 230-group total cross sections and the sum of partial cross sections for all 423 isotopes in the ENDF/B-VII.1 library.**

3.2.2 Benchmark Tests

The benchmark test cases in the MCC3_verification GitLab have been run using the E71 library. Table 3-4 shows the eigenvalues resulted from both the E70 and E71 libraries. Differences in eigenvalues are observed, with a maximum discrepancy of up to 267 pcm (jezebel), which can be attributed to changes in isotopic cross sections between the E70 and E71 data. Among the test cases, a k-infinitive (hereafter k-inf) difference of 4,727 pcm was observed for the 'newgroupstructure' case, which was caused by significant changes in the Cl^{35} cross sections in the E71 data. This discrepancy is expected, as the limited Reich-Moore resonance cross sections for Cl^{35} were not accurately processed in the current E71 library.

Table 3-4 Changes in k-effective between E70 and E71 MC^2-3 libraries in the benchmark problems from the MC^2-3 GitLab repository.

Case	k-inf		Δk
	E70	E71	pcm
check_n2n_Be9	1.80180	1.80123	-57
check_xe135 [a)]	1.24347	1.24265	-82
doppler_run1 region 1	2.02354	2.02297	-57
region 2	2.02266	2.02210	-56
region 3	2.02198	2.02142	-56
dummy_out	1.47669	1.47616	-53
gamma_pmatrxgamiso_run1	1.53951	1.53970	19
gammalib_read_bin	1.82858	1.82721	-137
godiva	2.26157	2.26046	-111
hexassm2d_ring01_test01	1.20872	1.21013	141
hexassm2d_ring02_test01	1.44938	1.45114	176
hexassm2d_ring02_test02	1.32614	1.32775	161
hexcell2d_ring01_test01	1.86834	1.86746	-88
hexcell2d_ring01_test02	1.86837	1.86749	-88
hexcell3d_ring01_test01	1.79018	1.79055	37
hfg_lowPu_run1	1.24229	1.24189	-40
hfg_lowPu_run2	1.24179	1.24139	-40
hom_1region	1.09714	1.09683	-31
hom_2region	1.24229	1.24189	-40
hom_2region_pwxs_run1	1.40909	1.40827	-82
hom_leakage	1.28712	1.28709	-3
iso_th232	0.61500	0.61611	111
jezebel	2.96456	2.96189	-267
lumpedFP_out	1.47665	1.47613	-52
lumpedFP_editISOTXS_run1	1.29563	1.29744	181
newgroupstructure [b)]	1.33165	1.37892	4727
oneD_cylinder	1.31112	1.31235	123
oneD_cylinder_dummy	0.02922	0.02921	-1
oneD_cylinder_gamma_94gl_21ggv2	1.82238	1.82250	12
oneD_cylinder_gamma_94gl_21ggv2_CRB10	0.70148	0.70132	-16

oneD_cylinderHFG_run1	1.31111	1.31235	124
oneD_cylinderHFG_run2	1.31054	1.31178	124
oneD_cylinder_homregion_start2	0.05287	0.05277	-10
oneD_cylinder_regioneditMacro	1.30199	1.30350	151
oneD_cylinder_spatial_hom_disabled	0.68763	0.68740	-23
oneD_slab	1.25528	1.25690	162
oneD_slab_homregion_all1	0.75786	0.75680	-106
reccell2d_1x1_test01	1.86836	1.86747	-89
reccell2d_1x1_test02	1.34357	1.34572	215
reccell2d_2x2_test01	1.80960	1.80903	-57
reccell2d_4x4_test01	1.57630	1.57605	-25
twodant_step1 region 1	1.24534	1.24586	72
region 2	1.23927	1.23971	65
region 3	0.33268	0.33342	74
region 4	0.32764	0.32834	70

a) The change of -1356 pcm occurred from library v1.7.
b) Cl^{35} is included in the test case.

3.2.3 Homogeneous Mixture Problems

Several homogeneous models have been devised, considering both fresh and depleted fuel compositions. These models include uranium-only, HEU based UO_2 fuel from CEFR, UPu-10Zr fuel from VTR, and High-Assay Low-Enriched Uranium (HALEU) in U-10Zr form from ARC100. Additionally, simplified homogeneous cases were created with only the major isotopes included, as shown in Table 3-5. A total of 16 cases were calculated using MC^2-3 at a temperature of 300 K. Reference solutions were generated using Serpent2.

For the three simplified FA compositions, only the major isotopes are included, while many minor isotopes are ignored. The CEFR and ARC100 fuel assembly compositions are for fresh fuel, while the VTR fuel assembly composition is for depleted fuel with many fission products included.

For the results shown in Table 3-6, it can be seen that MC^2-3 with the E71 library provides accurate k-inf values for most cases, with differences within 44 pcm, compared to corresponding Monte Carlo solutions. However, the k-inf difference for the 88 wt% enriched uranium case is relatively large, at -90 pcm, compared to the 11 pcm difference obtained with the E70 library. This discrepancy may be attributed to the limitations of the Narrow Resonance (NR) approximation. Further investigation into this issue will be necessary. Overall, the change in k-inf values from Serpent2 between the E70 and E71 data is consistent with the change in k-inf values from MC^2-3 between the two libraries.

To examine the impact of Doppler broadening for the E71 library, MC^2-3 and MCNP6 calculations were conducted for the VTR composition at various temperatures ranging from 300 K to 1200 K. The comparison results, shown in Table 3-7, indicate that the Doppler broadening effects are well represented at the selected temperatures, with differences within 10 pcm.

Table 3-5 Compositions of simplified homogeneous cases

Isotope	Atom Number Density (10^{24}/cm^3)				
	88 wt% Uranium	12 wt% Uranium	CEFR Simplified FA	VTR Simplified FA	ARC100 Simplified FA
U^{235}	5.00000E-03	7.00000E-04	5.21124E-03	3.76161E-04	2.28062E-03
U^{238}	7.00000E-04	5.00000E-03	2.87195E-03	7.82273E-03	1.22511E-02
Pu^{239}				1.48286E-03	
Pu^{240}				6.01603E-04	
Na^{23}			9.11988E-03	7.90904E-03	8.89573E-03
Cr^{52}			2.16952E-03	2.20917E-03	1.66968E-03
Cr^{53}				2.50509E-04	1.85492E-04
Fe^{54}				1.03652E-03	8.03708E-04
Fe^{56}			8.77107E-03	1.62707E-02	1.22564E-02
O^{16}			1.61664E-02		

Table 3-6 Comparison of multiplication factors between Serpent2 and MC^2-3 with MCC_LIB and PENDF_LIB for various homogeneous compositions at 300 K

Case	Serpent2 [1] k-infinitive			MC^2-3 [2] Δk (MC^2-3 – Serpent2), pcm		
	E70	E71	Δk [3]	E70	E71	Δk [3]
88 wt% enriched U	2.24185	2.24174	-11	11	-90	-112
12 wt% enriched U	1.40865	1.40837	-28	45	-9	-82
CEFR FA	1.92720	1.92844	124	35	-15	74
CEFR simplified FA	1.96381	1.96392	11	33	-12	-34
EBR2 composition 1	1.93764	1.94018	254	24	-28	202
EBR2 composition 1 simple	1.99397	1.99623	226	6	-36	184
EBR2 composition 2	1.98801	1.98953	152	3	-29	120
EBR2 composition 2 simple	2.03601	2.03759	158	12	-44	102
VTR composition	1.63238	1.63237	-1	34	-29	-64
VTR composition simple	1.67223	1.67506	283	22	-7	254
ARC100 composition	1.36008	1.36098	90	78	30	42
ARC100 composition simple	1.40046	1.40091	45	49	1	-3

[1] Standard deviation ≤ 0.00009
[2] MC^2-3 v3.3.3
[3] [k-inf (E71) – k-inf (E70)], pcm

Table 3-7 Comparison of multiplication factors between MCNP6 and MC^2-3, for VTR (depleted) fuel composition, using ENDF/B-VII.1 data library at different temperatures

Temperature, K	MCNP6 k-inf [1)]	MC^2-3 k-inf	Δk (pcm) [2)]
300	1.68828	1.68818	-10
600	1.68464	1.68470	-6
900	1.68283	1.68285	2
1200	1.68159	1.68163	4

1) [k-inf (MC^2-3) – k-inf (MCNP6)] × 10^5 pcm

2) $\sigma \leq 0.00002$

3.2.4 Benchmark Core Problems

In this section, a set of benchmark problems of the MC^2-3 Git repository were selected to verify the BG (typical 230 energy groups in these calculations) cross section generated by MC^2-3. These benchmark problems include cases with simple geometry, such as Godiva and Jezebel LANL benchmarks, which are un-reflected bare fuel spheres. For these problems with simple geometry, the two-dimensional (2D) code TWODANT was used for neutron transport calculations with the BG cross sections produced by MC^2-3.

The benchmark problems with more complex geometries, such as three-dimensional (3D) whole core models of ABTR and ZPPR-15, are included in the test suite. For the problems with complex geometries, the 3D code DIF3D was employed for neutron transport calculations, using either hexagonal or cartesian meshes along with the BG cross section provided by MC^2-3. For all the benchmark problems, MCNP6 results are used as references for both E70 and E71 neutron libraries. The comparison of k-effective (hereafter k-eff) values between MCNP6 and DIF3D (or TWODANT) is listed in Table 3-8.

The comparison of k-eff values in Table 3-8 indicates that the solutions from MC^2-3/DIF3D or TWODANT and MCNP6 solutions generally agree well within 200 pcm, with exceptions for ZPPR-21A, ZPPR-21F, and ABTR cases. These outliers are illustrated in Figure 3.5. For these cases, relatively large differences of up to -285 pcm were observed with both E70 and E71 libraries, suggesting that the issues do not stem from the E71 library. However, Further investigation is needed to determine the causes of these discrepancies.

In addition, as illustrated in Figure 3.6, the trends in k-eff changes between E70 and E71 data are consistent for both MCNP6 and MC^2-3/DIF3D or TWODANT. However, in a few LANL cases (Flattop-25, Jezebel-240, Jezebel-233, and Jezebel), the trend in k-eff changes is opposite. These cases involve bare sphere geometries with very hard spectra, where k-eff values are significantly influenced by threshold energy cross sections and fission spectra. Further investigation is required to determine the causes of these opposite trends in k-eff values.

Table 3-8. Comparison of eigenvalues between Monte Carlo (MCNP) and MC²-3/DIF3D or TWODANT for fast system benchmark problems.

Case		Monte Carlo [a]		MC²-3/DIF3D or TWODANT Δk, pcm [b]	
		E70	E71	E70	E71
LANL	Flattop-25	1.00293	1.00279	27	-7
	Flattop-Pu	1.00091	1.00093	-44	-115
	Flattop-23	0.99941	0.99884	-116	-118
	Godiva	0.99991	0.99983	33	4
	Jezebel-240	0.99993	1.00003	45	-30
	Jezebel-233	0.99969	0.9997	-3	19
	Jezebel	0.99999	0.99984	33	-17
	Big Ten	0.99540	0.99531	143	83
ZPR-6	6A	0.99603	0.99553	70	66
	7	0.98689	0.98642	84	85
ZPPR-21	A	0.99879	0.99607	-276	-271
	B	0.99314	0.99053	-52	-32
	C	0.99914	0.99669	-190	-188
	D	1.00329	1.00114	69	74
	E	1.00521	1.00312	-77	-85
	F	1.00652	1.00441	-260	-285
ZPPR-15	L15	0.99936	0.99844	13	54
	L16	0.99522	0.99428	7	57
	L20	0.99736	0.99643	86	89
Monju	Hom (Hex-Z)	0.99706	0.99663	187	200
BFS	55-1	0.97527	0.97469	119	100
	73-1	0.99567	0.99496	132	118
	75-1	0.99372	0.99305	46	27
ABTR		1.03519	1.03181	-178	-223

a) MCNP6 standard deviation ≤ 0.00007

b) Δk = (MC – MC²-3/DIF3D or TWODANT), pcm

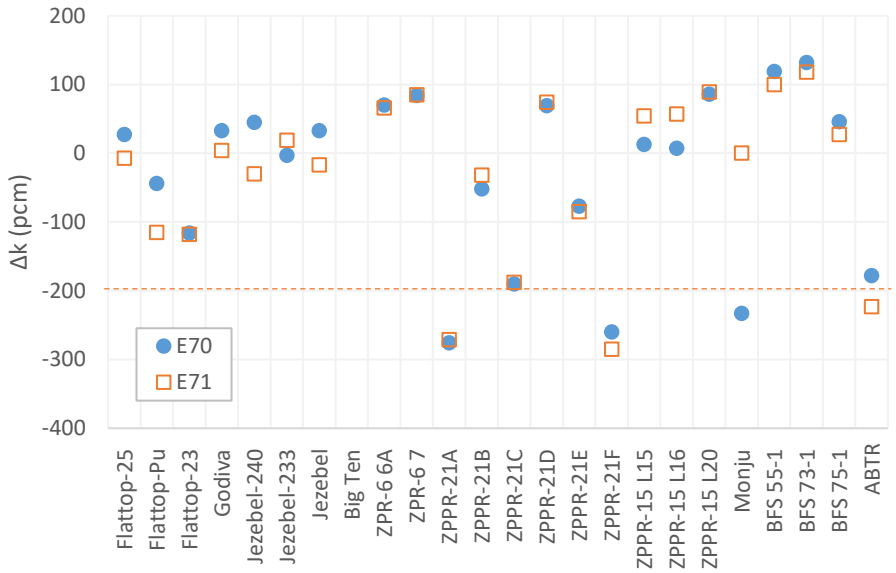

Figure 3-5 **Comparison of Eigenvalues between MC²-3 and Monte Carlo Solutions for Fast Reactor Benchmark Problems, using ENDF/B-VII.0 and -VII.1 data**

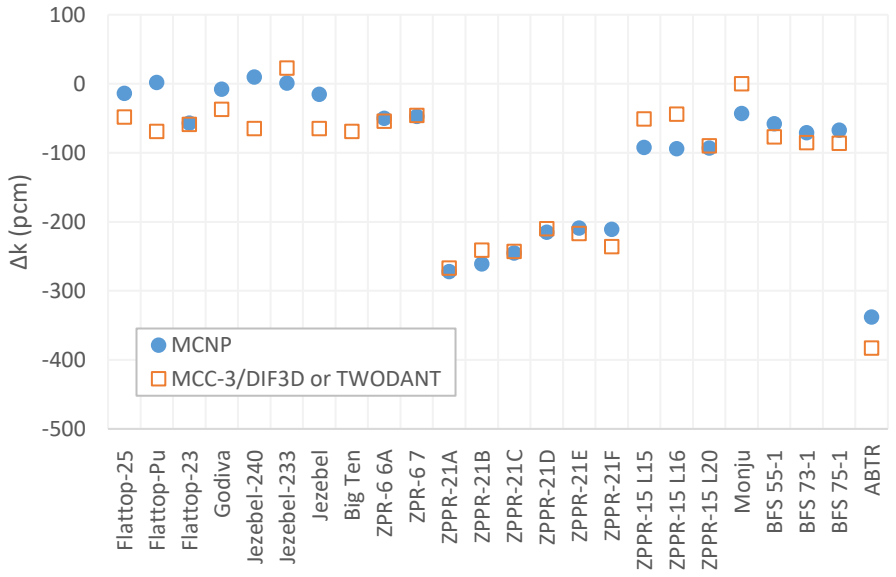

Figure 3-6 **Changes in Eigenvalues between ENDF/B-VII.0 and -VII.1 libraries, resulted from MC²-3 and Monte Carlo Solutions for Fast System Problems.**

4. ENDF/B-VII.1-based Gamma Library

The MC^2-3 gamma library generated using the ENDF/B-VII.1 data has been verified by solving a zero-dimensional (0D) homogeneous problem for each isotope in the gamma library and comparing the results with those from MCNP6.2. This section describes the MC^2-3 gamma library generation procedure and verification results.

4.1 Gamma Library Generation

The MC^2-3 gamma library for 423 isotopes using ENDF/B-VII.1 data was generated following the same procedure outlined in the previous report [11] for the verification and validation of the MC^2-3 gamma library the ENDF/B-VII.0 data. The procedure is briefly described here, and detailed information is available in the report [11].

Figure 4.1 shows the overall data flow for generating the MC^2-3 gamma library. The PreGAMMA code [12] prepares NJOY inputs for all isotopes and creates a batch script to run all NJOY inputs. After NJOY processing, the code also prepares the input for the GenGAMMA code [12] and calls it via the batch script to generate the final MC^2-3 gamma library. PreGAMMA also directly processes Q values for delayed beta and photon from an ENDF/B data file and generates delayed photon production matrix from JENDL-4.0 [13]. GenGAMMA then post-processes the NJOY outputs to generate partial kinetic energies (kinetic energies of secondary charged particles for each neutron reaction), photon production yield and cross section matrix, and photon total KERMA factor and photon interaction cross sections, all of which are stored in the MC^2-3 gamma library. In this work, NJOY99.v396 was used.

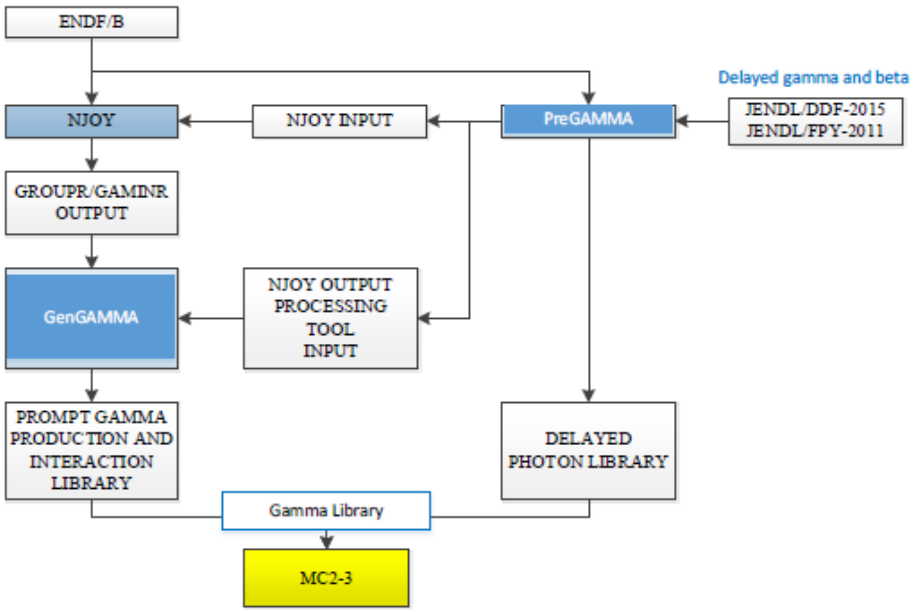

Figure 4-1 **Overall data flow for the generation of the MC^2-3 gamma library.**

It is important to note that the Q values for the delayed beta and gamma data are identical for ENDF/B-VII.0 and ENDF/B-VII.1, except for additional isotopes in ENDF/B-VII.1. This is because the delayed beta data are available for only a few important isotopes in ENDF/B-VII.0, so the ENDF/B-VII.1 data was used for those isotopes in ENDF/B-VII.0. The delayed gamma data come from JENDL.

4.2 Verification

The established procedure was verified by comparing its results with MCNP for isotope-wise problems and the EBR-II benchmark problem. The isotope-wise verification consists of two types of problems: an eigenvalue problem and a fixed source problem. In the eigenvalue problem, Pu^{238} is mixed with the target isotope to provide a fission source. However, the presence of Pu^{238} complicates a consistent comparison of the photon heating rate of the target isotope due to different treatments of fluorescent photons between the MC^2-3/DIF3D/GAMSOR and MCNP procedures. Thus, the fixed source problem without Pu^{238} was additionally solved to improve confidence in the photon heating results of the target isotopes. The EBR-II problem was selected as an integral test.

4.2.1 Isotope-wise Eigenvalue Problem

Isotopic verification tests were conducted for all isotopes in the MC^2-3 library by comparing MC^2-3/DIF3D/GAMSOR results for homogeneous problems with MCNP results. For each isotope, all data in the MC^2-3 gamma library, except for delayed components, were compared with MCNP data. In order to isolate the effect of the gamma library data, the neutron flux solution from MCNP was used as input for the DIF3D/GAMSOR calculations. To eliminate transport calculation errors, a 0D homogeneous problem was solved for each isotope.

For fissionable isotopes, a single isotope problem was created with only the isotope of interest. For non-fissionable isotopes, the problem consisted of the isotope of interest and Pu^{238}. In order to minimize the impact of the fission source material, Pu^{238} was chosen as the accompanying isotope because it does not have photon production data in ENDF/B VII.1 and did not introduce noticeable errors in its own problem. The following computational procedure was used for the isotopic verification tests in this section.

1) MCNP
    - Solve an eigenvalue problem in an infinite homogeneous medium with a total number density of 1/barn-cm. For fissionable isotopes, the homogeneous problem consists solely of the isotope of interest. For non-fissionable isotopes, the composition includes a mixture of the isotope of interest and Pu^{238}. In order to accurately capture the energy deposited by fluorescent photons, the detailed photon physics model was employed using the options listed in Table 4-1.

Table 4-1. MCNP Photon Physics Options for the Consistent Comparison

Input Parameter	Value	Description
emcpf	100 MeV	Upper energy limit for detailed photon physics treatment
ides	1	Bremsstrahlung generation off
nocoh	1	Coherent scattering off
ispn	0	Photonuclear particle production off
nodop	1	Photon Doppler broadening off

2) MC^2-3

- Generate ISOTXS, PMATRX, and GAMISO files by solving the same eigenvalue problem.

3) DIF3D

- Step 1: convert the 230-group MCNP neutron spectrum into the RTFLUX format of DIF3D; calculate the photon source with GAMSOR using the RTFLUX and PMATRX files; save the photon source into a FIXSRC file.
- Step 2: solve the fixed-source gamma problem with DIF3D using the GAMISO and FIXSRC files; save the 94-group photon spectrum into a GTFLUX file.
- Step 3: edit the neutron and gamma heating results with the SUMMAR module of DIF3D using the PMATRX, RTFLUX and GTFLUX files.

The neutron heat generation rate, photon heat generation rate, and photon production rate were compared to examine the neutron KERMA factor, the photon production matrix, and the photo-atomic cross section and photon KERMA factor. The errors for neutron heating and photon production rates of target isotopes are shown in Figure 4-2 and Figure 4-3. Results generally match well, except for a few isotopes. Figure 4-4 shows the errors in the photon heating rate for target isotopes, while Figure 4-5 shows the same quantity for a material (a target isotope + Pu^{238}). For the target isotope only, large errors up to -10% are observed for intermediate mass nuclides, whereas good agreement is observed for material-wise comparison. This is due to different treatments of fluorescent photons between DIF3D and MCNP, which will be explained in detail later in this section. Table 4-2 shows the list of isotopes whose relative errors are greater than $\pm$5% in neutron heating, material photon heating, and photon production rate when compared to MCNP6.2 results. Only 10 out of 423 isotopes exhibit these significant errors, with 5 isotopes showing errors larger than $\pm$10%.

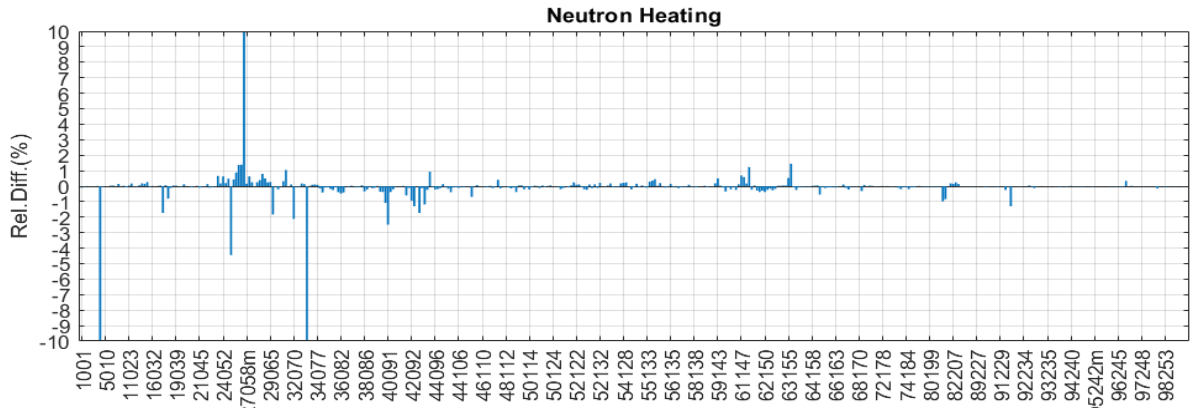

Figure 4-2 **Relative differences (%) in neutron heat generation rate of target isotopes compared to MCNP results.**

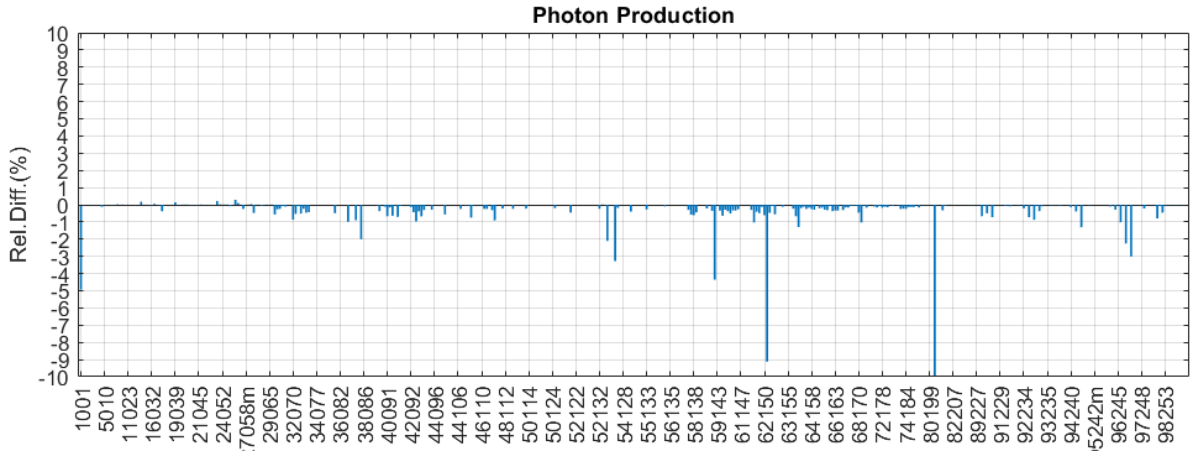

Figure 4-3 **Relative differences (%) of prompt photon production rate of target isotopes compared to MCNP results.**

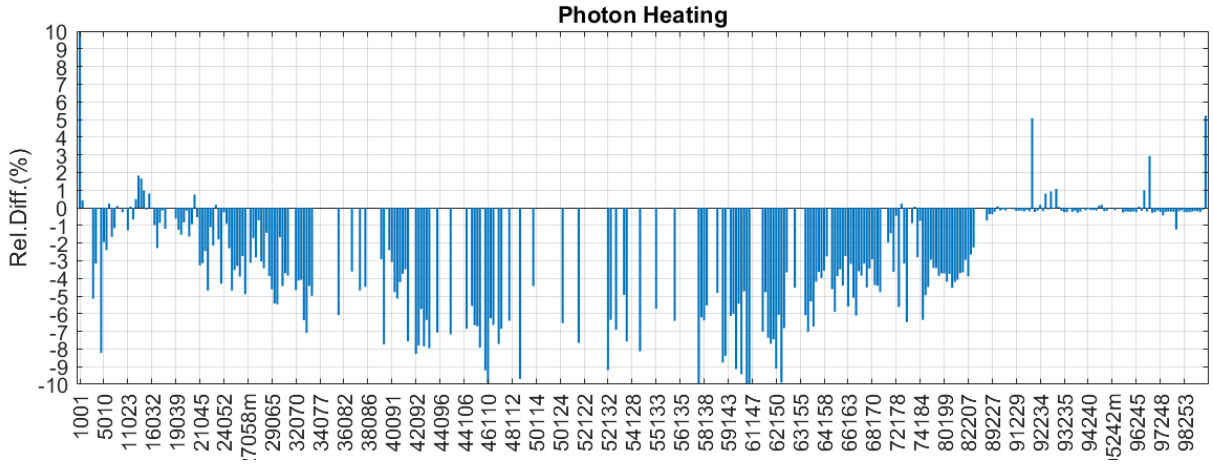

Figure 4-4 Relative differences (%) in photon heat generation rate of target isotopes compared to MCNP results.

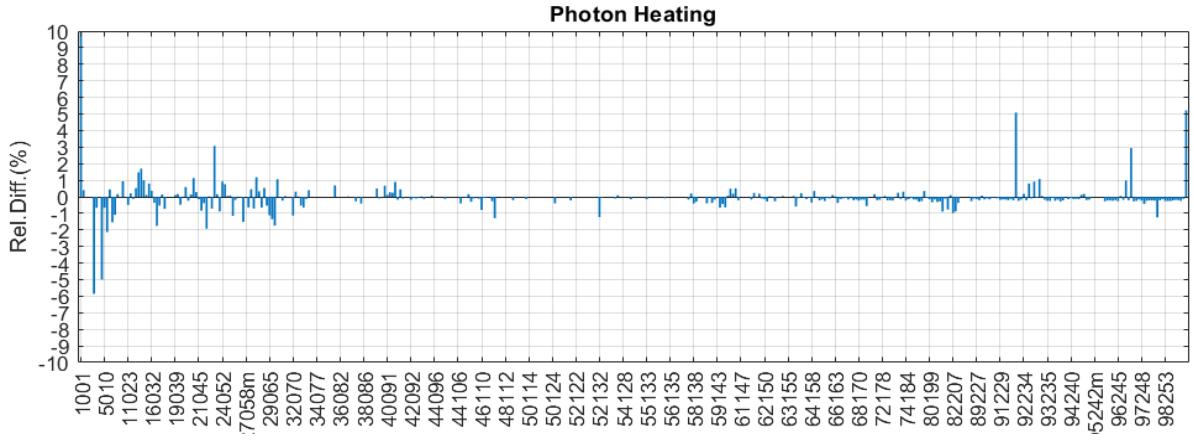

Figure 4-5 Relative differences (%) in photon heat generation rate of a material (target isotope + Pu-238) compared to MCNP results.

Table 4-2. Isotopes with Relative Differences of Greater Than 5% in Neutron Heat Generation Rate, Photon Production Rate, and Photon Heat Generation Rate.

Isotope	Neutron Heating	Photon Heating	Photon Production
H^{1}	-0.1	108.6	-4.9
Li^{6}	0.0	-5.9	0.0
Be^{7}	-37.6	-	-
Be^{9}	0.0	-5.0	-0.1
Co^{58}	168.3	-1.5	-0.2
As^{74}	-79.7	-0.1	-0.5
Sm^{151}	-0.2	-0.3	-9.1
Hg^{201}	0.0	-0.2	-13.5
U^{231}	0.0	5.1	0.0
Fm^{255}	0.0	5.2	0.0

To understand the reason for the different error trends shown in Figure 4-4 and Figure 4-5, a detailed analysis was performed using the Nd^{150} problem whose error is -11.79% in Figure 4-4. Table 4-3 compares the photon heating rates of Nd^{150} for the Nd^{150} + Pu^{238} problem across different calculation modes. Before explaining the results in Table 4-3, it should be reminded that the MC^2-3/DIF3D/GAMSOR tool assumes the local deposition of fluorescent photon energy via the photon KERMA factor, while MCNP explicitly considers the production and transports of fluorescent photons if the detailed photon physics option is enabled. For the simple photon physics option, the contribution of fluorescent photon to the photon heating rate is ignored. This distinction can be understood from Figure 4-6 which shows the heating number (photon heating rate per photo-atomic reaction) of Nd^{150} calculated by the GAMINR module of NJOY for the MC^2-3 gamma library and the ACER module of NJOY for the MCNP library. The difference between the green and blue lines is the energy of Nd^{150} fluorescent photon. Since the energy of fluorescent photon

energy is considered in the photon heating number in the MC^2-3/DIF3D/GAMSOR procedure, they are not transported but assumed to deposit their energy locally. In contrast, MCNP transports fluorescent photons and considers their energy deposited by other interactions. Figure 4-7 illustrates this distinction. The MCNP simple physics photon flux and DIF3D flux match well without fluorescent photons, while the MCNP detailed physics photon flux includes fluorescent photon contributions at the K-shells of Pu^{238} and Nd^{150} atoms.

Back to Table 4-3, the two MC^2-3/DIF3D/GAMSOR calculations that use DIF3D photon flux and MCNP simple physics photon flux gave almost identical results. This is because fluorescent photons do not contribute to both photon fluxes, as discussed above. In these two values, only the energy of Nd^{150} fluorescent photons is considered via the photon heating number. Meanwhile, MCNP simple physics solution is about -3% smaller than the MC^2-3/DIF3D/GAMSOR results because the energy of fluorescent photon is completely ignored. The MCNP detailed physics result is about +12% higher than the MC^2-3/DIF3D/GAMSOR results because it accounts for the energy of both Nd^{150} and Pu^{208} fluorescent photons, which are deposited through interactions with Nd^{150}. This analysis indicates that it is not feasible to make a fully consistent comparison of each individual isotope's photon heating rate in a mixture problem.

Table 4-3. Comparison of Nd^{150} Photon Heating Rates from Different Calculation Modes for the Eigenvalue Problem of Nd^{150} + Pu^{238}.

Calculation Mode	ARC calculation		MCNP calculation	
	MC^2-3 + DIF3D flux	MC^2-3 + MCNP Simple physics flux	Simple physics	Detailed physics
Photon heating (MeV)	0.4078	0.4076	0.3947	0.4623
Fluorescent photon's energy considered	Nd^{150}	Nd^{150}	None	Nd^{150} + Pu^{238}

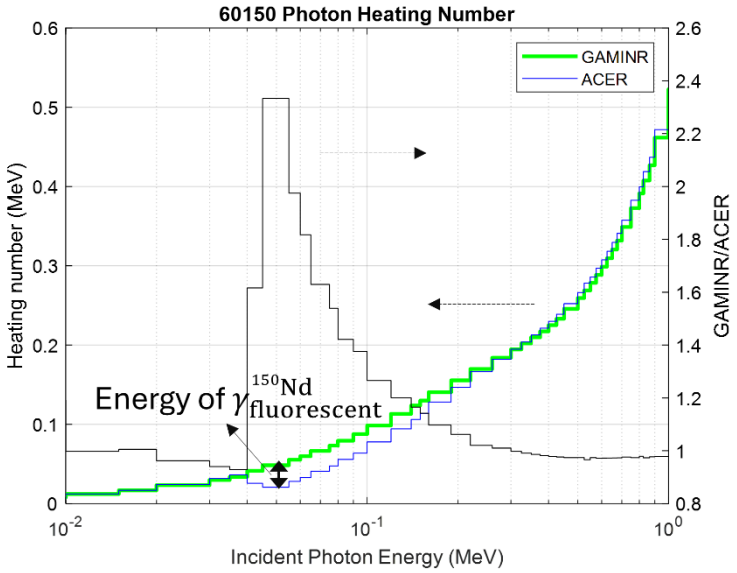

Figure 4-6. Different photon heating values (MeV/reaction) of Nd generated by GAMINR and ACER.

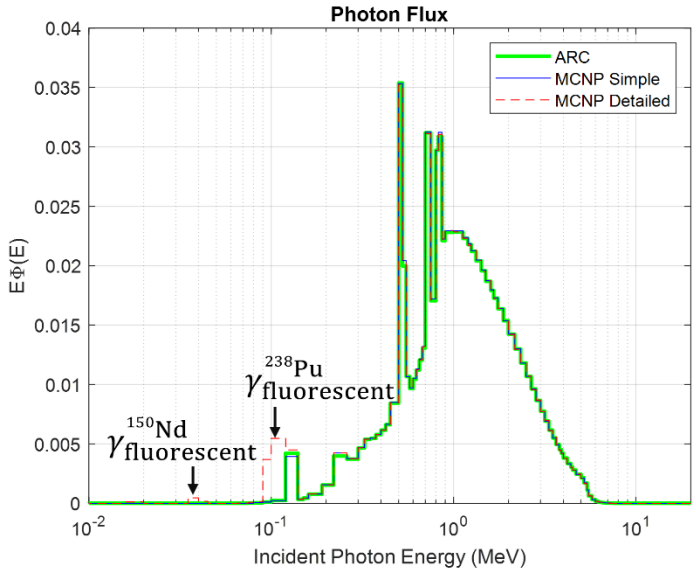

Figure 4-7. Photon flux comparison of DIF3D, MCNP simple physics option, and MCNP detailed physics option.

4.2.2 Isotope-wise Fixed Source Problem

For a better comparison of the photon heating results, a single-isotope problem was solved by performing a fixed-source photon transport calculation. A 94-group fixed photon source was prepared from an infinite SFR fuel composition as shown in Figure 4-8 and used for all isotopes. For MCNP, a photon-only problem (mode p) was solved with the detailed photon physics option using the photon source from Figure 4-8 normalized to unity. Then, the f6 tally was used to edit the photon heating spectrum. For DIF3D, a FIXSRC file containing the same photon source and a 94-group GAMISO file were provided to DIF3D with the fixed-source mode for all isotope problems. Then, the DIF3D photon flux was edited and multiplied to gamma KERMA factors to calculate the photon heating spectrum.

Figure 4-9 shows the results, showing excellent agreement for most isotopes including Nd^{150}. For Nd^{150}, the error is 0.04%. Figure 4-10 compares the photon flux spectrum and photon heating spectrum from DIF3D and MCNP on the left and right plots, respectively, for the Nd^{150} problem. The photon flux matches well, except for fluorescent photon of Nd^{150} at around 0.04 eV. Even though photon heating rate shows noticeable deviations, their sum matches within 0.04%. While this holds for most intermediate and heavy isotopes, significant deviations are observed for light isotopes. The biggest error of 26% is observed for hydrogen. Figure 4-11 shows the same plots as Figure 4-10 for hydrogen. Due to very small capture cross sections, most photon sources are slowed down without being absorbed, resulting in a very unrealistic photon flux as shown on the left of Figure 4-11. The photon flux deviation directly translates to photon heating deviation, as shown on the right of Figure 4-11. Nevertheless, such a large error in this type of spectrum shape would not be of concern. The observations for the most of remaining isotope problems, whose spectra are closer to realistic ones, strengthen the confidence in the accuracy of the photon data.

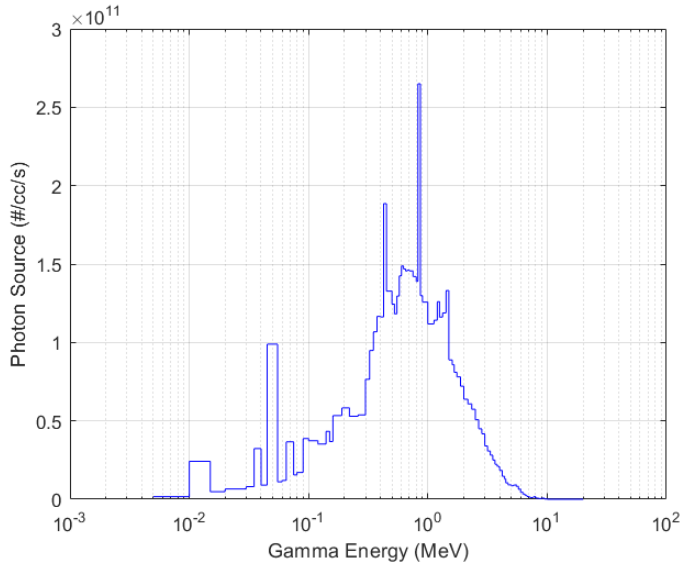

Figure 4-8. Fixed photon source used for the fixed source problems of all isotopes.

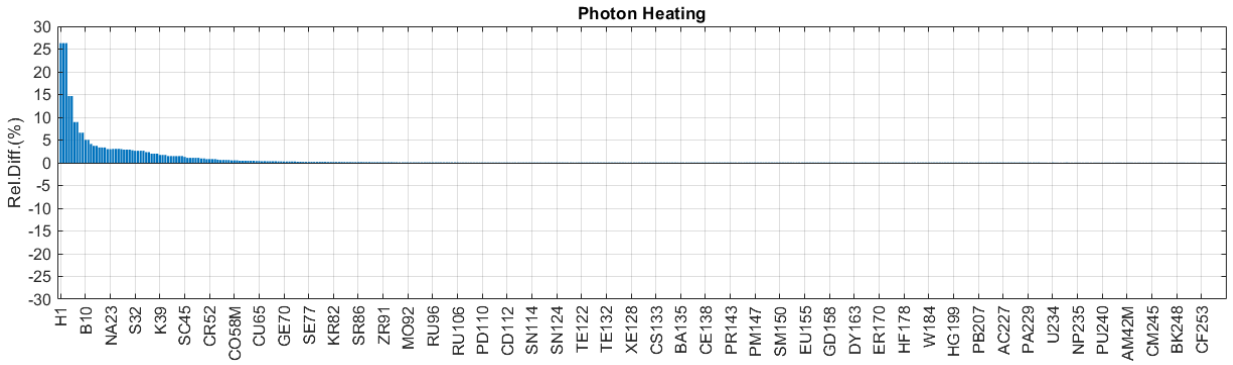

Figure 4-9. Relative differences (%) in photon heat generation rate of target isotopes compared to MCNP results for fixed source photon problems.

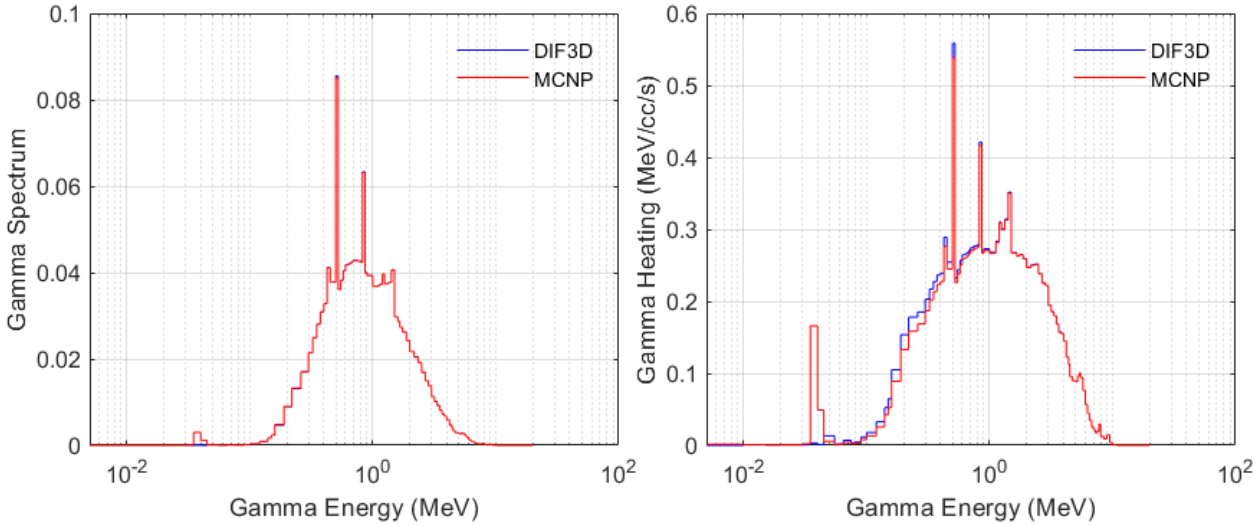

Figure 4-10. Comparison of gamma flux spectrum (left) and gamma heating spectrum (right) from DIF3D and MCNP for the Nd problem.

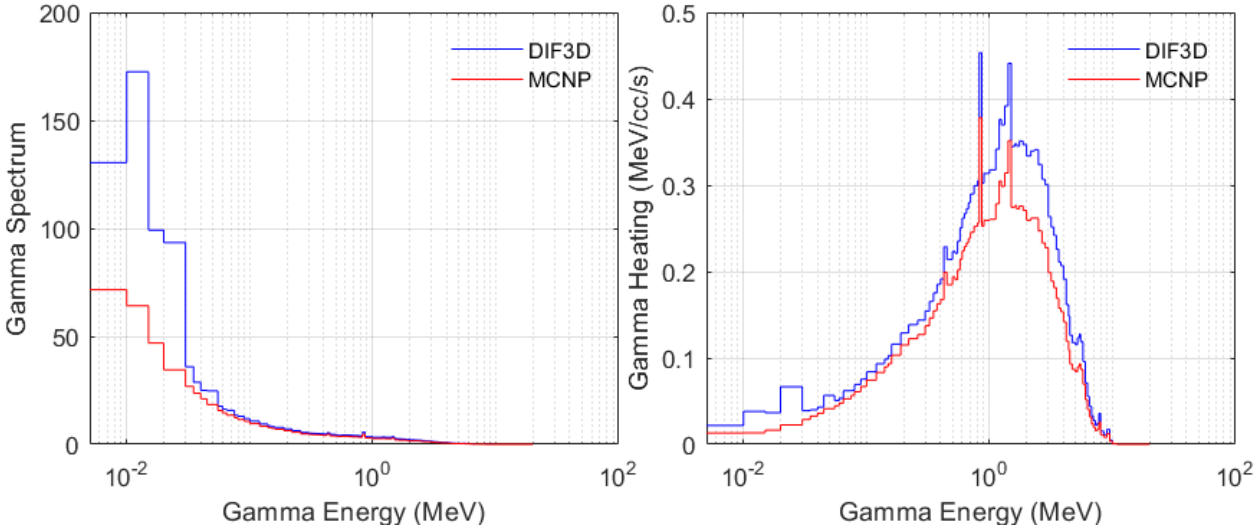

Figure 4-11. Comparison of gamma flux spectrum (left) and gamma heating spectrum (right) from DIF3D and MCNP for the H problem.

4.2.3 EBR-II SHRT Run 138B Benchmark Problem

The EBR-II SHRT benchmark problem based on Run 138B core configuration [14] was solved. The Run 138B core consists of 71 regular driver fuel assemblies, 13 half-worth (HW) driver fuel assemblies, 8 control rod and 2 safety assemblies, 6 structure (steel dummy) assemblies, and 3 fuel test and 3 material test assemblies. Figure 4-6 shows the core layout. The detailed 3D core configuration can be found in Ref. [14].

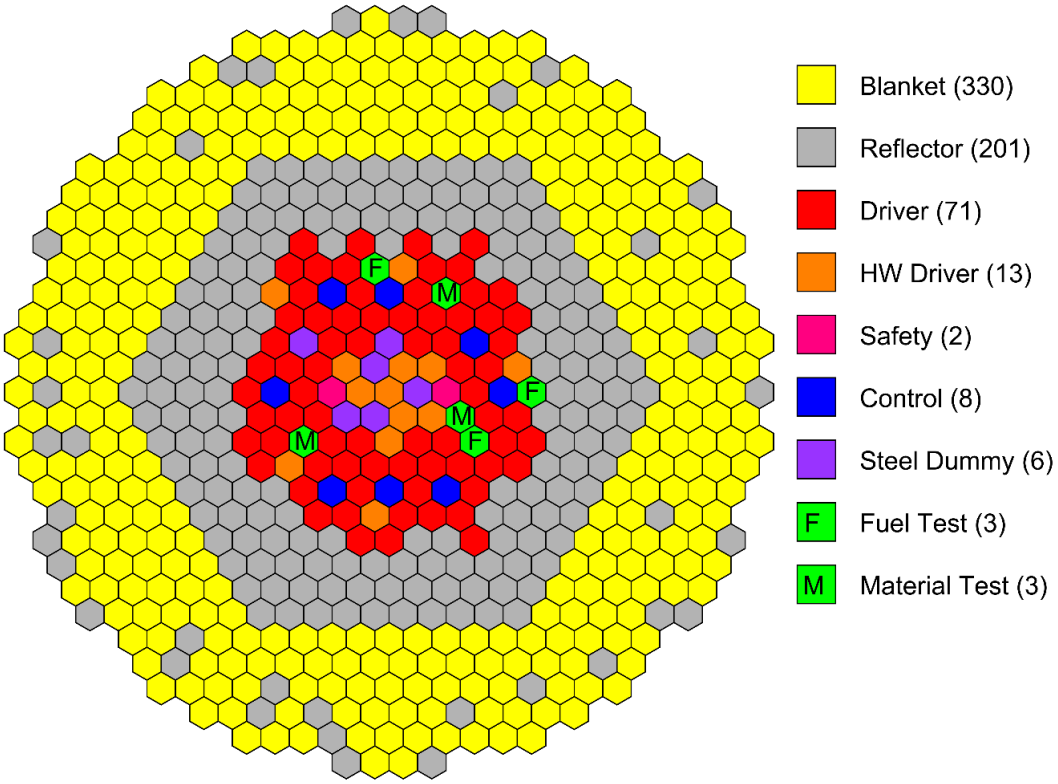

Figure 4-12 **EBR-II SHRT Run 138B core configuration.**

The MCNP reference solution was obtained with a homogenized assembly core model. The coupled neutron and gamma transport simulations were conducted using 100,000 particles per cycle with 200 inactive and 1000 active cycles. Figure 4.6 shows the relative assembly power distributions obtained from MCNP. The RMS and maximum values of the standard deviation of total assembly powers were 0.41% and 1.28%, respectively. Using the MC^2-3 code, 33-group neutron and 21-group gamma cross sections were generated. Region-dependent 33-group neutron cross sections were generated using an UFG spectrum that was obtained from a whole-core transport calculation with TWODANT. For the 21-group gamma cross sections, it was found that the region-to-region spectral transition effect is minimal so that there is no need to perform a TWODANT gamma transport calculation [11]. For gamma production cross sections and neutron KERMA factors, the delayed part was excluded by using the `l_prompt = true` option in MC^2-3 because the MCNP simulation only accounts for the prompt part.

DIF3D calculations for neutron transport were performed using various combinations of angular and anisotropic scattering orders. P3P3 (P3 angular approximation and P3 anisotropic scattering approximation), P5P3, P5P5, and P7P3 were tested. However, using the angular approximation order higher than P3 for gamma transport produced a wrong gamma flux solution. Thus, P3P3 was used for gamma transport in all cases. A slightly modified version of DIF3D was used to allow different orders for neutron and gamma transport calculations. The spatial polynomial approximation order was set to 6 for the angular flux, 4 for the source, and 1 for the leakage.

Table 4-3 compares the DIF3D eigenvalue solutions with the MCNP reference value. For ENDF/B-VII.0, only the P5P3 option was used, yielding an eigenvalue error of -255 pcm. Switching to ENDF/B-VII.1 results in a similar error level, at -314 pcm. Note that the ENDF/B-VII.0 result differs slightly from the value reported in Ref. [11], as the code and library used in this work are slightly different from the one used in Ref. [11]. In the ENDF/B-VII.1 results, it is evident that increasing the angular approximation order improves the eigenvalue, while increasing the anisotropic scattering order higher than 3 does not. Specially, using the P7 angular approximation provides a 501 pcm improvement over the P3 option, resulting in an error of -121 pcm.

Table 4-4. Eigenvalue Result for the EBR-II SHRT Run 138B Benchmark Problem

ENDF/B-VII.0			ENDF/B-VII.1		
Code	k-eff	Δk (pcm)	Code	k-eff	Δk (pcm)
MCNP	0.99378	$\pm$6 (S.D.)	MCNP	0.98802	$\pm$6 (S.D.)
			DIF3D – P3P3	0.98180	-622
DIF3D – P5P3	0.99123	-255	DIF3D – P5P3	0.98488	-314
			DIF3D – P5P5	0.98492	-310
			DIF3D – P7P3	0.98681	-121

Figure 4.7 to Figure 4.10 illustrate the relative differences in neutron, photon and total power distribution results of DIF3D using ENDF/B-VII.0 with the P5P3 option (for neutron transport), ENDF/B-VII.1 with P3P3, P5P3, and P7P3 options, respectively, compared to the MCNP result. The relative error trends are similar; there are higher errors in the steel dummy and material test assemblies where no fission power occurs, and in the reflector assemblies except those in the last ring and in assemblies in the first ring of the blanket region. Results of ENDF/B-VII.0 and ENDF/B-VII.1 are very similar, and using higher angular approximations gradually reduces errors. This is more clearly shown in the error statistics averaged over each assembly type in Table 4-4 as well. The P5P3 calculation, which is realistic considering the computational time, produces good results with average error levels below 2% in all regions.

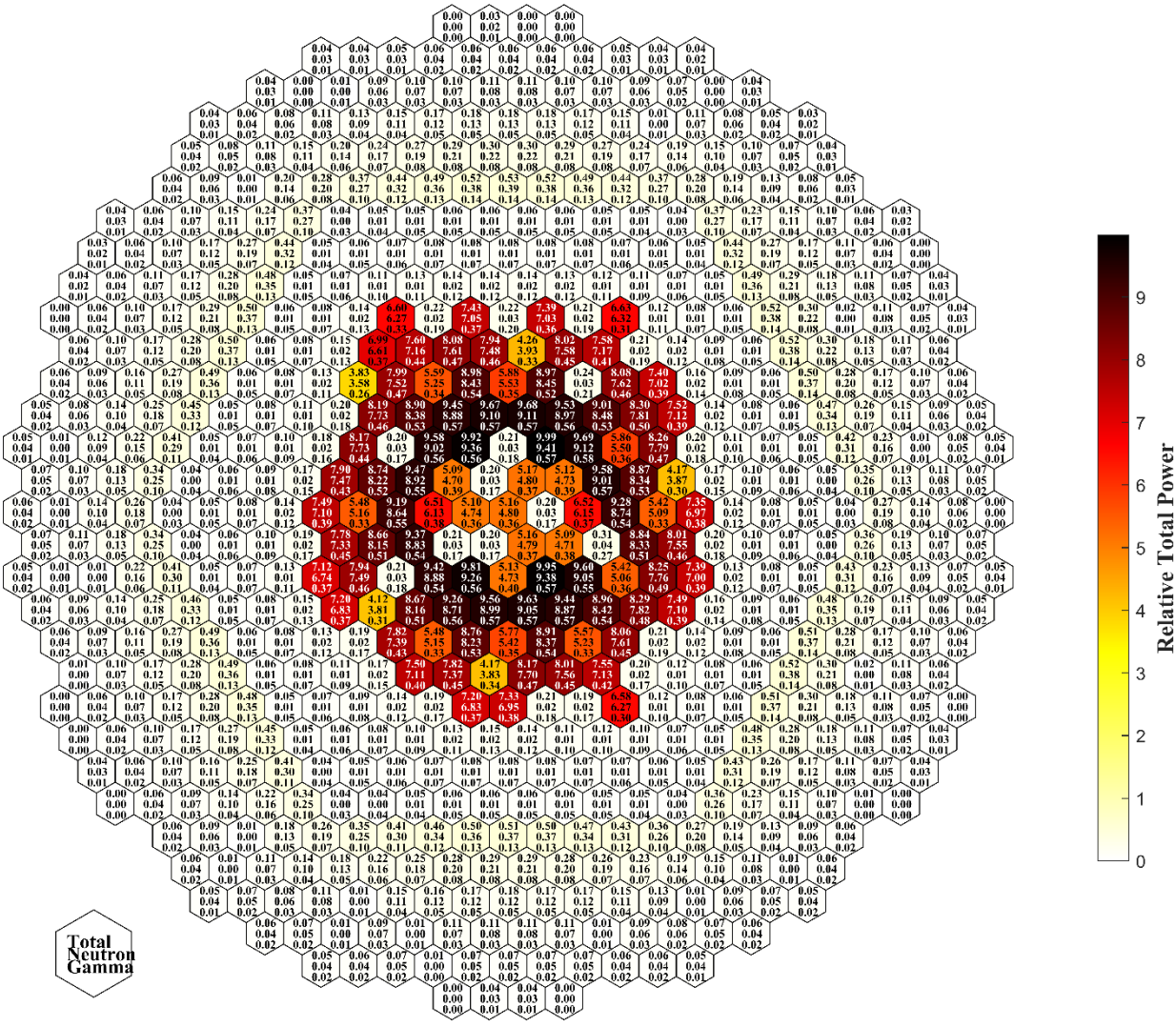

Figure 4-13 **Relative assembly power distributions of the EBR-II SHRT Run 138B benchmark problem obtained from MCNP simulation.**

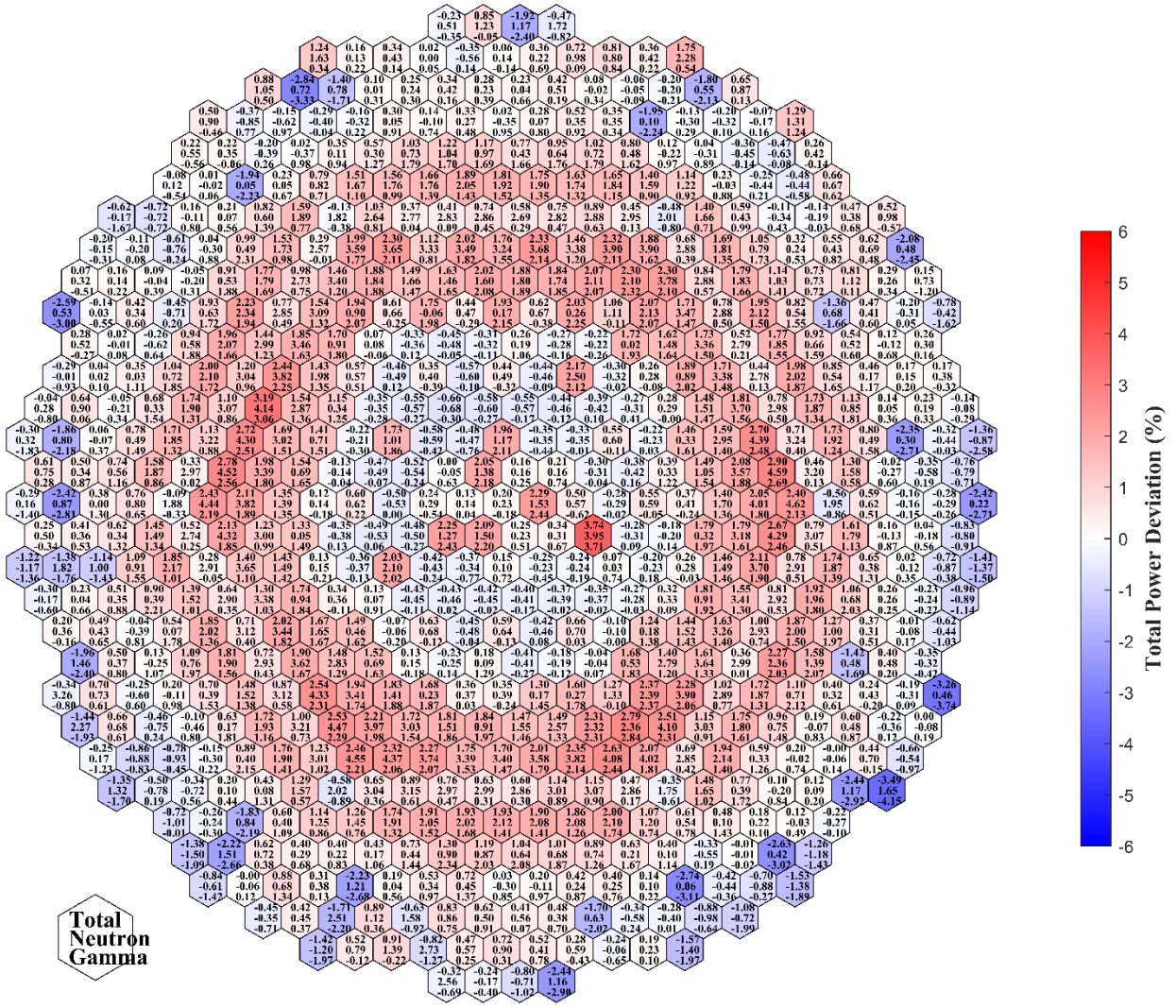

Figure 4-14 **Comparison of DIF3D power distribution using ENDF/B-VII.0 and the P5P3 option for neutron transport calculation with MCNP result.**

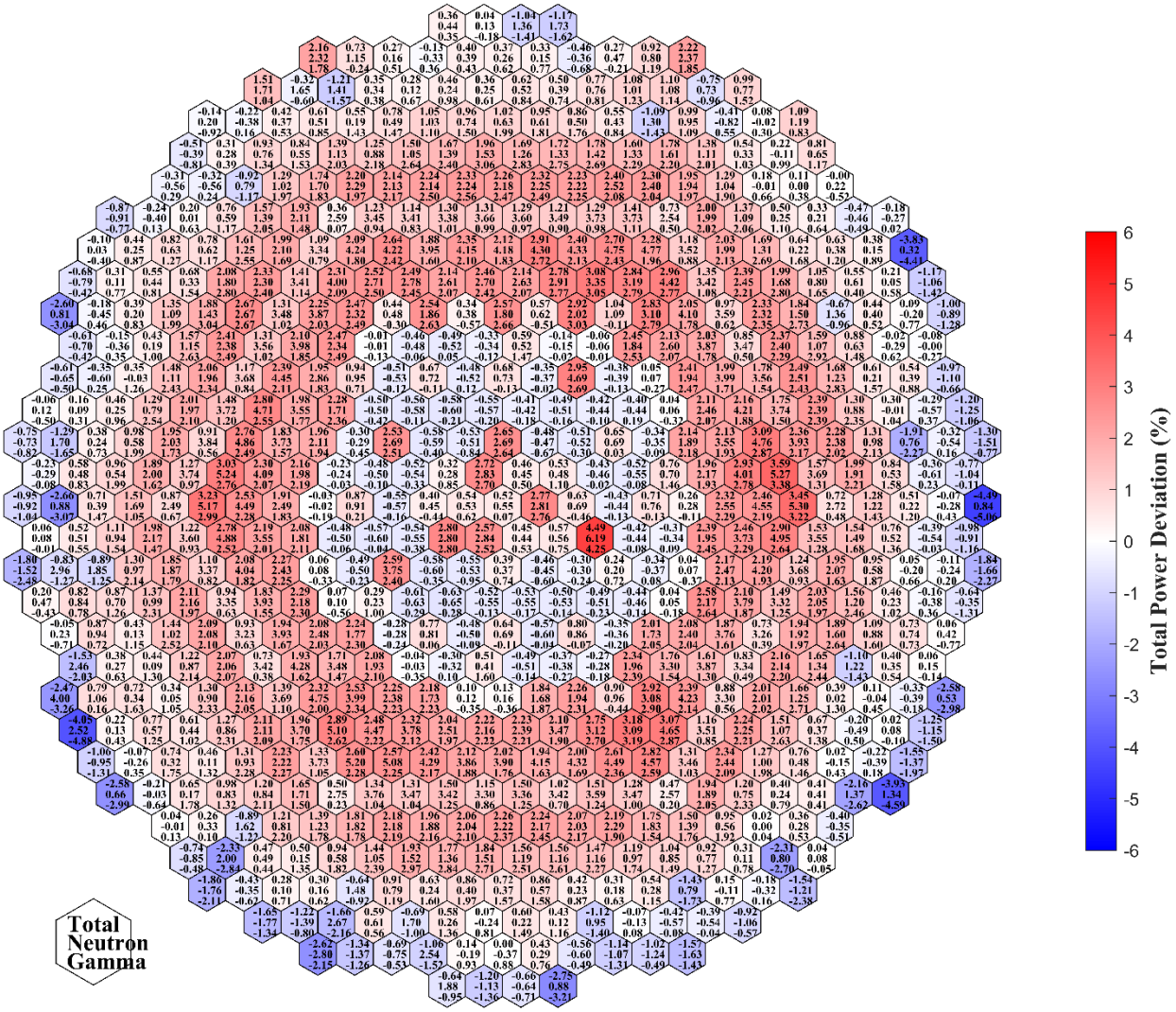

Figure 4-15 **Comparison of DIF3D power distribution using ENDF/B-VII.1 and the P3P3 option for neutron transport calculation with MCNP result.**

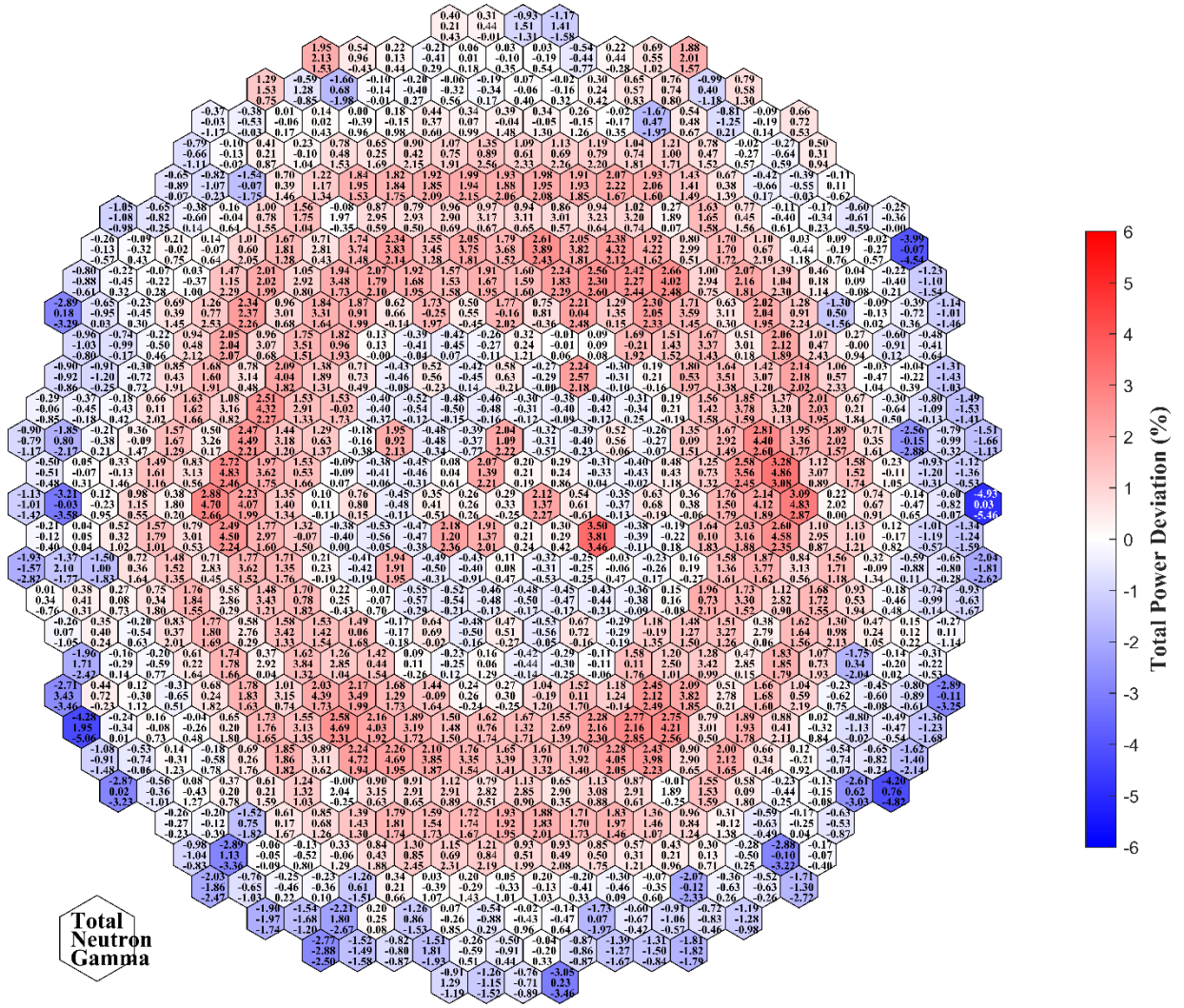

Figure 4-16 **Comparison of DIF3D power distribution using ENDF/B-VII.1 and the P5P3 option for neutron transport calculation with MCNP result.**

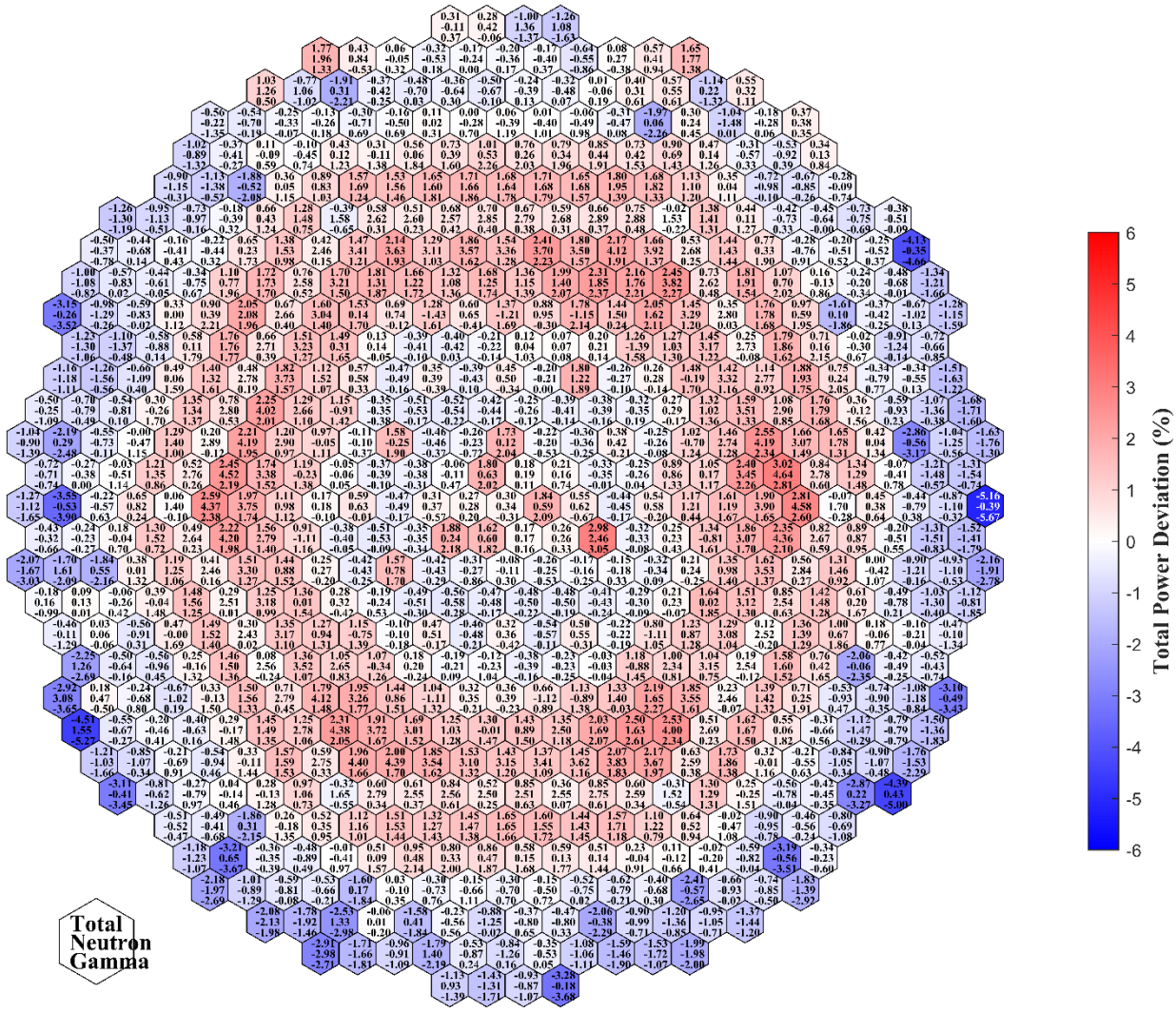

Figure 4-17 **Comparison of DIF3D power distribution using ENDF/B-VII.1 and the P7P3 option for neutron transport calculation with MCNP result.**

Table 4-5. Summary of Assembly Power Deviations (%) of DIF3D Solutions from MCNP Reference

Assembly	ENDF/B-VII.0		ENDF/B-VII.1					
	P5P3[a]/P3P3[b]		P3P3/P3P3		P5P3/P3P3		P7P3/P3P3	
	RMS	Min/Max	RMS	Min/Max	RMS	Min/Max	RMS	Min/Max
Total	1.20	-3.49/3.74	1.53	-4.49/4.49	1.30	-4.93/3.50	1.22	-5.16/3.02
Fuel	0.86	-0.66/3.74	1.12	-0.63/4.49	0.85	-0.55/3.50	0.76	-0.56/2.98
Inner Reflector	1.62	-0.58/3.19	2.05	-0.01/3.59	1.66	-0.08/3.28	1.43	-0.39/3.02
Outer Reflector	1.16	-2.59/0.62	1.21	-2.75/0.87	1.46	-3.05/0.40	1.66	-3.28/0.31
Blanket	1.05	-3.49/2.27	1.35	-4.49/2.67	1.18	-4.93/2.34	1.16	-5.16/2.05
Control	1.04	-0.48/2.17	1.37	-0.53/2.95	1.05	-0.39/2.24	0.83	-0.26/1.80
Structure*	0.59	-0.40/1.73	0.88	-0.53/2.53	0.67	-0.48/1.95	0.55	-0.48/1.58

a: neutron transport, b: gamma transport

5. Conclusions

Last year, the ENDF/B-VII.0 (E70) library of MC^2-3 was thoroughly reverified and updated to meet the commercial grade dedication (CGD) requirements of the TerraPower Natrium project. The preliminary version of the ENDF/B-VII.1 (E71) library was generated incorporating many of the resolutions identified during the verification of the E70 library. This year, the E71 library has been rigorously regenerated and verified to ensure it meets the CGD requirements.

The final version of the E71 neutron library includes 11 data files: MCCF1 – MCCF8 generated from ETOE2, MCCF9 (isotopic fission spectra and total cross sections) and MCCF10 (isotopic P0 and P1 scattering matrices) generated from NJOY and Python scripts, and ADELAY (isotopic delayed neutron data) generated from ENDF data using a Python script.

The E71 library was verified through comparisons using 230-group cross sections generated from NJOY and 230-group resolved resonance cross sections generated from MC^2-3 with the PENDF library, as well as comparisons of total cross sections with the sum of partial cross sections. Isotopes with issues identified during the verification process have mostly been corrected by updating ETOE2.

Additional verifications were conducted with numerous homogeneous mixture problems generated from typical fast reactor compositions, including CEFR, EBR-II, VTR, and ARC100. These verifications demonstrated that k-eff solutions from MC^2-3 and Monte Carlo codes agree well within 44 pcm, except for the 88 wt% enriched U^{235} case, which showed a k-eff difference of 90 pcm. The comparison of k-eff values between MCNP6 and MC^2-3/DIF3D or TWODANT across 24 fast reactor benchmark problems indicated that they generally agree well within 200 pcm, with a few exceptions showing differences of up to -285 pcm. It was observed that the trends in k-eff changes between E70 and E71 data are consistent for both MCNP6 and MC^2-3/DIF3D or TWODANT. Therefore, we can conclude that the E70 neutron library was accurately generated even though a few to several isotopes require further investigation to reduce errors.

On the other hand, the E71 gamma library has also been generated, including partial kinetic energies, gamma production yields and cross section matrices, and gamma total KERMA factors and interaction cross sections for all isotopes. The delayed beta and gamma data remain unchanged, except for the addition of new isotopes in the E71 data, as the Q values for delayed beta and gamma were previously generated using E71 data and the delayed gamma production yield were produced using JENDL-4.0. Testing of the E71 gamma library using the EBR-II core problem indicated that DIF3D calculations with the P5P3 option produced good results, with average errors below 2% in all regions of the EBR-II core.

Finally, the E71 neutron library v1.1 and the gamma library v1.0 have been saved in the MC^2-3 library GitLab repository, and the relevant data used for verification tests have been stored in the MC2-3 verification GitLab repository.

REFERENCES

1. C. H. Lee and W. S. Yang, "MC^2-3: Multigroup Cross Section Generation Code for Fast Reactor Analysis," *Nucl. Sci. Eng.*, **187**, 268 (2017).
2. C. H. Lee, Y. S. Jung, and W. S. Yang, "MC^2-3: Multigroup Cross Section Generation Code for Fast Reactor Analysis," ANL/NE-11/41 Rev 3, Argonne National Laboratory (2022)
3. R. E. Alcouffe et al., "User's Guide for TWODANT: a Code Package for Two-dimensional, Diffusion-accelerated, Neutral-particle Transport, Revision 1," LA-10049-M, October (1984).
4. M. B. Chadwick et al., "ENDF/B-VII.0: Next Generation Evaluated Nuclear Data Library for Nuclear Science and Technology," *Nuclear Data Sheets*, **107**, 2931-3060 (2006).
5. Z. Zhong and C. H. Lee, "Improvement and Verification of the ENDF/B-VII.0 based MC^2-3 Library," ANL/NSE-23/43 Rev.3, Argonne National Laboratory, February (2024).
6. M. B. Chadwick et al., "ENDF/B-VII.1: Nuclear Data for Science and Technology: Cross Sections, Covariances, Fission Product Yields and Decay Data," *Nuclear Data Sheets*, **111**, 12, 2887-2996 (2011).
7. R. E. MacFarlane, D. W. Muir, R. M Boicourt, et al., "The NJOY Nuclear Data Processing System, version 2016," LA-UR-17-20093, Los Alamos National Laboratory, July (2018).
8. C. J. Werner et al., "MCNP User's Manual Code Version 6.2," LA-UR-17-29981, Los Alamos National Laboratory, October (2017).
9. M.A. Smith, E.E. Lewis, and E.R. Shemon, "DIF3D-VARIANT 11.0, A Decade of Updates," ANL/NE-14/1, Argonne National Laboratory (2014).
10. C. H. Lee, H. Park, and Z. Zhong, "Recent Updates in ETOE-2 and MC^2-3," ANL/NSE-21/75, September (2021).
11. H. Park, W. S. Yang, M. Smith and C. H. Lee. "Verification and Validation Tests of the Gamma Library of the ARC Software Package (Rev.1)," Argonne National Laboratory, ANL/NSE-19/22 Rev.1, September 30 (2022).
12. C. H. Lee, B. K. Jeon, and W. S. Yang, "User Manual for MC2 -3 Gamma Library Generation, Rev. 0," ANL/NSE-18/12, Argonne National Laboratory, October 10 (2018).
13. K. Shibata et al., "JENDL-4.0: A New Library for Nuclear Science and Engineering," *J. Nucl. Sci. Technol.*, **48**(1), 1-30 (2011).
14. T. Fei, A. Mohamed and T. K. Kim, "Neutronics Benchmark Specifications for EBR-II Shutdown Heat Removal Test SHRT-45R - Revision 1," ANL-ARC-228 Rev. 1, Argonne National Laboratory (2013).

Appendix A.1 Verification of Resolved Resonance Cross Sections in the MC^2-3 ENDF/B-VII.1 Library

Table A-0-1 Comparison of the 230-group resolved resonance cross sections generated from MC^2-3 with ENDF/B-VII.1 MC^2-3 and PENDF libraries for all isotopes

Isotope ID	Resolved Resonance Type	Maximum error (%) of cross section			
		total	capture	Scattering	Fission
NA22_7	MLBW	0.11	5.59	0.58	
NA23_7	MLBW	0.45	4.11	0.45	
MG24_7	MLBW	2.21	1.75	2.21	
MG25_7	MLBW	1.61	4.86	1.61	
MG26_7	MLBW	0.33	5.87	0.33	
AL27_7	RM	2.10	1.63	2.17	
SI28_7	RM	24.31	31.16	24.94	
SI29_7	RM	0.46	16.06	0.45	
SI30_7	RM	0.84	94.28	0.83	
S32__7	MLBW	5.70	10.01	5.72	
S33__7	MLBW	0.16	384.42	0.18	
S34__7	MLBW	1.69	4.03	1.70	
CL37_7	RM	13.20	12.88	13.38	
AR36_7	MLBW	0.60	0.37	0.60	
AR38_7	MLBW	0.82	5.00	0.82	
AR40_7	RM	42.11	2.86	42.61	
K39__7	RM	20.62	7.09	20.69	
K41__7	RM	3.25	3.65	3.64	
CA40_7	MLBW	3.55	14.83	3.56	
CA42_7	MLBW	10.39	69.08	10.34	
CA43_7	MLBW	3.81	6.29	3.69	
CA44_7	MLBW	3.48	3.21	3.55	
CA48_7	MLBW	0.59	8.52	0.59	
SC45_7	MLBW	0.70	1.96	0.70	
TI46_7	MLBW	6.21	1.67	6.24	
TI47_7	MLBW	2.66	3.05	2.66	
TI48_7	RM	7.96	4.29	7.96	
TI49_7	MLBW	0.51	1.49	0.52	
TI50_7	MLBW	4.31	8.53	4.30	
V50__7	MLBW	1.68	0.78	1.70	
V51__7	RM	16.22	145.94	16.22	
CR50_7	RM	10.49	10.81	10.49	
CR52_7	RM	2.61	9.07	2.63	
CR53_7	RM	9.70	9.66	9.70	
CR54_7	RM	11.34	2.59	11.62	
MN55_7	RM	13.26	12.24	13.29	
FE54_7	RM	8.12	9.33	8.12	
FE56_7	RM	9.89	16.56	9.89	
FE57_7	RM	13.62	119.55	13.74	
FE58_7	RM	8.44	6.42	8.52	
CO58_7	MLBW	0.40	0.37	0.49	
CO58_7	MLBW	0.40	0.37	0.49	
CO59_7	RM	5.85	7.35	5.63	

NI58_7	RM	5.74	19.02	5.75	
NI59_7	MLBW	2.16	2.53	2.26	
NI60_7	RM	32.64	19.86	33.46	
NI61_7	MLBW	3.41	7.58	3.42	
NI62_7	MLBW	0.78	2.89	0.78	
NI64_7	MLBW	1.96	9.66	1.96	
CU63_7	RM	1.88	7.76	1.92	
CU65_7	RM	4.66	6.72	4.66	
ZN64_7	MLBW	0.33	1.05	0.34	
ZN66_7	MLBW	0.28	0.79	0.29	
ZN67_7	MLBW	0.27	0.54	0.31	
ZN68_7	MLBW	0.50	3.30	0.50	
ZN70_7	MLBW	0.35	2.40	0.35	
GA69_7	MLBW	0.12	0.66	0.12	
GA71_7	MLBW	0.35	0.49	0.35	
GE70_7	MLBW	5.52	3.85	5.60	
GE72_7	MLBW	0.35	2.82	0.36	
GE73_7	MLBW	0.74	6.37	0.52	
GE74_7	MLBW	0.35	1.12	0.35	
GE76_7	MLBW	0.25	2.35	0.25	
AS74_7	MLBW	0.37	0.52	0.04	
AS75_7	MLBW	0.17	0.40	0.09	
SE74_7	MLBW	0.25	7.69	0.31	
SE76_7	MLBW	0.24	0.85	0.24	
SE77_7	MLBW	0.22	0.42	0.19	
SE78_7	MLBW	0.10	1.34	0.10	
SE80_7	MLBW	1.46	2.01	2.85	
SE82_7	MLBW	0.20	2.05	0.20	
BR79_7	MLBW	0.22	0.44	0.08	
BR81_7	MLBW	0.08	0.88	0.11	
KR78_7	MLBW	0.08	0.40	0.05	
KR80_7	MLBW	0.17	1.85	0.25	
KR82_7	MLBW	0.31	0.40	0.32	
KR83_7	MLBW	0.23	0.34	0.09	
KR84_7	MLBW	0.26	2.41	0.26	
KR85_7	MLBW	0.16	6.54	0.38	
KR86_7	MLBW	1.29	76.60	1.29	
RB85_7	MLBW	0.05	0.42	0.05	
RB86_7	MLBW	0.09	0.40	0.09	
RB87_7	MLBW	0.18	1.05	0.18	
SR84_7	MLBW	0.07	0.62	0.07	
SR86_7	MLBW	0.39	1.65	0.40	
SR87_7	MLBW	0.41	1.34	0.08	
SR88_7	MLBW	2.24	3.21	2.24	
Y89__7	MLBW	0.33	2.68	0.33	
Y90__7	MLBW	27.44	71.35	27.15	
ZR90_7	MLBW	0.22	3.39	0.22	
ZR91_7	MLBW	0.15	0.49	0.15	
ZR92_7	MLBW	0.49	2.48	0.49	
ZR93_7	MLBW	0.11	1.21	0.10	
ZR94_7	MLBW	0.54	3.30	0.54	
ZR96_7	MLBW	1.32	2.70	1.33	
NB93_7	SLBW	0.12	0.32	0.10	

NB94_7	MLBW	0.27	0.88	0.10	
MO92_7	MLBW	0.17	2.48	0.17	
MO94_7	MLBW	0.17	2.85	0.17	
MO95_7	MLBW	0.16	0.61	0.13	
MO96_7	MLBW	0.32	3.32	0.38	
MO97_7	MLBW	0.10	0.52	0.03	
MO98_7	MLBW	0.19	2.40	0.13	
MO1007	MLBW	0.06	1.80	0.07	
TC99_7	MLBW	0.43	0.47	0.06	
RU99_7	MLBW	0.46	2.41	0.03	
RU1007	MLBW	0.08	3.58	0.08	
RU1017	MLBW	0.51	1.78	0.03	
RU1027	MLBW	0.04	1.99	0.04	
RU1037	MLBW	0.15	0.46	0.03	
RU1047	MLBW	0.37	0.70	0.38	
RH1037	MLBW	0.63	0.64	0.13	
RH1057	SLBW	0.39	0.37	0.46	
PD1027	MLBW	0.05	0.43	0.03	
PD1047	MLBW	0.05	1.40	0.06	
PD1057	MLBW	0.17	0.42	0.03	
PD1067	MLBW	0.08	1.31	0.08	
PD1077	MLBW	0.97	4.00	0.05	
PD1087	MLBW	0.26	0.82	0.47	
PD1107	MLBW	0.08	1.36	0.09	
AG1077	MLBW	0.15	0.37	0.04	
AG1097	MLBW	0.59	0.57	0.93	
AG10M7	MLBW	0.66	1.20	0.03	
AG1117	MLBW	0.06	0.39	0.03	
CD1067	RM	1.76	1.04	1.80	
CD1087	RM	0.74	4.97	1.67	
CD1107	RM	3.20	4.02	2.83	
CD1117	RM	12.12	106.23	0.04	
CD1127	RM	1.49	2.72	2.42	
CD1137	MLBW	0.42	0.43	0.24	
CD1147	RM	0.62	5.02	1.04	
CD15M7	MLBW	0.83	4.66	0.04	
CD1167	RM	0.42	3.33	0.05	
IN1137	MLBW	0.44	0.53	0.20	
IN1157	MLBW	0.55	0.60	1.04	
SN1127	MLBW	0.07	0.81	0.03	
SN1137	MLBW	2.50	2.19	2.61	
SN1147	MLBW	0.07	1.61	0.04	
SN1157	MLBW	0.17	0.63	0.03	
SN1167	MLBW	0.08	2.79	0.08	
SN1177	MLBW	0.10	1.20	0.03	
SN1187	MLBW	0.05	2.77	0.05	
SN1197	MLBW	0.07	1.30	0.03	
SN1207	MLBW	0.05	2.76	0.05	
SN1227	MLBW	0.26	5.85	0.26	
SN1247	MLBW	2.38	3.65	2.38	
SN1257	MLBW	0.22	2.54	0.20	
SB1217	MLBW	0.21	1.48	0.03	
SB1237	MLBW	0.18	1.01	0.09	

SB1267	MLBW	1.01	2.36	0.06	
TE1227	MLBW	0.16	0.83	0.11	
TE1237	MLBW	0.37	2.65	0.55	
TE1247	MLBW	0.11	0.89	0.11	
TE1257	MLBW	0.08	0.78	0.07	
TE1267	MLBW	0.15	3.80	0.15	
TE1287	MLBW	0.12	3.07	0.12	
TE1307	MLBW	0.06	4.14	0.06	
TE1327	MLBW	0.20	3.23	0.20	
I127_7	MLBW	0.22	0.39	0.11	
I129_7	MLBW	0.11	0.71	0.06	
I130_7	MLBW	1.48	3.03	0.05	
XE1247	MLBW	0.65	0.62	6.24	
XE1267	MLBW	0.18	2.82	0.05	
XE1287	MLBW	0.10	1.58	0.10	
XE1297	MLBW	0.30	0.67	0.08	
XE1307	MLBW	0.08	2.52	0.08	
XE1317	MLBW	0.40	1.16	0.44	
XE1327	MLBW	0.07	2.66	0.07	
XE1347	MLBW	0.03	3.45	0.02	
XE1357	SLBW	0.32	0.57	0.20	
XE1367	MLBW	1.91	1.22	1.91	
CS1337	MLBW	0.34	0.56	0.07	
CS1347	MLBW	0.25	0.36	0.04	
CS1357	MLBW	0.10	0.38	0.03	
BA1307	MLBW	0.28	1.22	0.19	
BA1327	MLBW	0.17	0.40	0.19	
BA1337	MLBW	0.17	0.49	0.13	
BA1347	MLBW	0.43	0.78	0.48	
BA1357	MLBW	0.21	0.99	0.20	
BA1367	MLBW	0.29	2.54	0.29	
BA1377	MLBW	0.11	1.17	0.11	
BA1387	MLBW	0.27	4.09	0.27	
BA1407	MLBW	0.33	2.22	0.33	
LA1387	MLBW	0.30	0.43	0.12	
LA1397	MLBW	0.28	1.11	0.28	
LA1407	MLBW	11.34	76.67	6.51	
CE1367	MLBW	0.29	0.40	0.37	
CE1387	MLBW	0.09	0.43	0.09	
CE1397	MLBW	0.32	0.83	0.08	
CE1407	MLBW	0.28	2.56	0.28	
CE1417	MLBW	0.33	0.42	0.37	
CE1427	MLBW	5.35	123.23	5.37	
CE1437	MLBW	0.49	2.48	0.12	
PR1417	MLBW	10.68	1.09	10.92	
PR1427	MLBW	6.37	6.30	6.44	
PR1437	MLBW	3.53	0.41	4.77	
ND1427	MLBW	0.34	28.31	0.22	
ND1437	MLBW	0.24	1.37	0.24	
ND1447	MLBW	4.13	0.53	31.31	
ND1457	MLBW	0.32	0.37	0.32	
ND1467	MLBW	0.42	0.59	0.43	
ND1477	MLBW	0.16	0.41	0.08	

ND1487	MLBW	0.34	1.00	0.34	
ND1507	MLBW	0.14	0.64	0.14	
PM1477	MLBW	0.48	0.44	0.56	
PM48M7	SLBW	0.33	0.33	0.36	
PM1517	MLBW	0.56	0.50	0.66	
SM1447	MLBW	0.36	1.90	0.36	
SM1477	MLBW	0.36	0.41	0.50	
SM1487	MLBW	0.17	0.42	0.17	
SM1497	MLBW	0.85	0.84	1.35	
SM1507	MLBW	0.25	0.73	0.11	
SM1517	MLBW	0.46	0.46	0.53	
SM1527	MLBW	0.37	0.50	0.44	
SM1537	MLBW	0.79	0.74	1.15	
SM1547	MLBW	0.07	0.82	0.06	
EU1517	MLBW	0.52	0.52	1.34	
EU1527	MLBW	0.63	0.63	0.65	
EU1537	MLBW	0.57	0.57	0.43	
EU1547	MLBW	0.46	0.47	0.15	
EU1557	MLBW	0.58	0.56	1.01	
EU1577	MLBW	0.77	1.16	0.18	
GD1527	RM	5.26	6.19	0.25	
GD1537	RM	0.35	0.47	0.03	
GD1547	RM	5.15	6.10	5.95	
GD1557	RM	0.46	0.48	0.16	
GD1567	RM	3.86	4.51	0.36	
GD1577	RM	0.40	0.45	0.10	
GD1587	RM	6.32	6.92	0.83	
GD1607	RM	0.30	5.22	0.31	
TB1597	MLBW	0.37	0.77	0.06	
TB1607	MLBW	0.52	0.53	0.68	
DY1567	MLBW	1.54	1.28	2.23	
DY1587	MLBW	0.15	0.37	0.13	
DY1607	MLBW	0.45	0.45	0.11	
DY1617	MLBW	0.33	0.37	0.07	
DY1627	MLBW	0.38	0.95	0.49	
DY1637	MLBW	0.49	1.62	0.43	
DY1647	MLBW	0.27	0.56	0.11	
HO1657	MLBW	0.28	0.41	0.35	
HO66M7	MLBW	0.47	0.46	0.57	
ER1627	MLBW	0.21	0.40	0.05	
ER1647	MLBW	0.12	0.40	0.03	
ER1667	MLBW	0.09	0.40	0.04	
ER1677	MLBW	0.50	0.99	1.64	
ER1687	MLBW	0.05	0.45	0.05	
ER1707	MLBW	0.20	1.65	0.19	
TM1687	MLBW	0.59	0.61	0.75	
TM1697	MLBW	0.29	0.66	0.31	
TM1707	MLBW	2.05	3.57	0.26	
LU1757	MLBW	0.36	0.49	0.05	
LU1767	MLBW	0.58	0.60	0.05	
HF1747	MLBW	0.25	0.39	0.24	
HF1767	MLBW	0.45	0.39	0.52	
HF1777	MLBW	0.51	0.50	0.83	

HF1787	MLBW	0.28	1.64	0.41	
HF1797	MLBW	0.30	0.40	0.07	
HF1807	MLBW	0.08	0.86	0.08	
TA1817	MLBW	0.41	0.43	0.11	
TA1827	MLBW	0.30	0.44	0.24	
W180_7	MLBW	0.14	0.37	0.07	
W182_7	RM	0.37	0.72	0.17	
W183_7	RM	0.28	0.37	0.25	
W184_7	RM	1.49	4.63	1.54	
W186_7	RM	10.82	11.34	10.74	
RE1857	MLBW	0.55	0.37	2.90	
RE1877	MLBW	0.21	0.42	0.03	
IR1917	MLBW	0.57	0.56	1.54	
IR1937	MLBW	0.50	0.52	0.06	
AU1977	MLBW	0.43	0.47	0.28	
HG1967	MLBW	0.32	0.40	0.06	
HG1987	MLBW	0.18	0.40	0.05	
HG1997	MLBW	0.31	0.38	0.18	
HG2007	MLBW	0.12	0.52	0.11	
HG2017	MLBW	0.05	0.39	0.05	
HG2027	MLBW	0.16	0.47	0.16	
TL2037	MLBW	0.36	0.95	0.36	
TL2057	MLBW	0.23	3.10	0.23	
PB2047	MLBW	0.16	1.45	0.16	
PB2067	RM	2.15	3.26	2.15	
PB2077	RM	4.35	49.59	4.36	
PB2087	RM	0.37	3.90	0.37	
BI2097	MLBW	0.14	2.59	0.14	
RA2267	MLBW	0.67	1.59	0.07	
TH2287	MLBW	0.69	0.69	0.47	0.18
TH2297	MLBW	0.49	0.53	0.42	0.48
TH2307	MLBW	0.40	0.50	0.49	0.18
TH2327	RM	0.05	5.96	0.65	-
PA2317	RM	0.39	0.43	0.08	0.46
PA2327	MLBW	0.29	0.41	0.11	0.31
PA2337	RM	0.32	0.52	0.03	-
U232_7	MLBW	0.23	0.39	0.04	0.41
U233_7	RM	0.33	0.47	0.07	0.38
U234_7	MLBW	0.44	0.45	0.77	0.42
U235_7	RM	0.17	0.49	0.38	0.16
U236_7	MLBW	0.26	0.41	0.10	0.41
U237_7	MLBW	0.67	0.68	0.11	0.62
U238_7	RM	0.23	2.73	0.32	4.41
U239_7	SLBW	0.47	0.52	0.07	0.52
U240_7	SLBW	0.28	1.09	0.52	0.24
U241_7	SLBW	0.35	0.40	0.03	0.40
NP2367	MLBW	0.19	0.52	0.18	0.16
NP2377	MLBW	0.49	0.52	0.06	0.42
NP2387	MLBW	0.43	0.47	0.21	0.44
PU2367	MLBW	0.92	1.15	0.17	1.23
PU2387	MLBW	0.11	0.44	0.07	0.35
PU2397	RM	0.29	0.37	0.02	0.42
PU2407	MLBW	0.42	0.63	1.37	0.65

PU2417	RM	0.24	0.48	0.05	0.23
PU2427	MLBW	0.30	0.40	0.20	0.32
PU2437	SLBW	0.44	0.50	0.04	0.50
PU2447	MLBW	0.13	0.93	0.04	0.93
AM2417	MLBW	0.52	0.62	0.15	0.58
AM2427	MLBW	0.45	0.44	0.12	0.47
AM42M7	MLBW	0.27	0.37	0.20	0.25
AM2437	MLBW	0.43	0.52	0.09	0.71
CM2427	MLBW	0.09	0.37	0.05	0.37
CM2437	MLBW	0.46	0.49	0.08	0.48
CM2447	MLBW	0.20	0.40	0.12	0.36
CM2457	MLBW	0.34	0.45	0.07	0.35
CM2467	MLBW	0.09	0.39	0.02	0.38
CM2477	MLBW	0.54	0.57	0.17	0.55
CM2487	MLBW	0.20	0.80	0.24	0.79
CM2507	MLBW	0.37	0.33	0.45	0.33
BK2497	MLBW	0.47	0.62	0.11	0.61
CF2497	MLBW	0.36	0.37	0.72	0.36
CF2507	MLBW	0.79	0.77	1.48	0.77
CF2517	MLBW	1.61	2.99	0.33	3.17
CF2527	MLBW	0.27	0.65	0.05	0.80
ES2537	MLBW	1.51	1.62	1.94	0.06

Nuclear Science and Engineering Division
Argonne National Laboratory
9700 South Cass Avenue, Bldg. 208
Argonne, IL 60439-4842

www.anl.gov